metals

MDPI

Article

On the Nb_5Si_3 Silicide in Metallic Ultra-High Temperature Materials

Panos Tsakiropoulos

Department of Materials Science and Engineering, Sir Robert Hadfield Building, The University of Sheffield, Mappin Street, Sheffield S1 3JD, UK; p.tsakiropoulos@sheffield.ac.uk

Abstract: Refractory metal (RM) M_5Si_3 silicides are desirable intermetallics in metallic ultra-high temperature materials (UHTMs), owing to their creep properties and high Si content that benefits oxidation resistance. Of particular interest is the alloyed Nb_5Si_3 that forms in metallic UHTMs with Nb and Si addition. The choice of alloying elements and type of Nb_5Si_3 that is critical for achieving a balance of properties or meeting a property goal in a metallic UHTM is considered in this paper. Specifically, the different types of alloyed "normal" Nb_5Si_3 and Ti-rich Nb_5Si_3, namely "conventional", "complex concentrated" (CC) or "high entropy" (HE) silicide, in metallic UHTMs with Nb and Si addition were studied. Advanced metallic UHTMs with additions of RMs, transition metals (TMs), Ge, Sn or Ge + Sn and with/without Al and with different Ti, Al, Cr, Si or Sn concentrations were investigated, considering that the motivation of this work was to support the design and development of metallic-UHTMs. The study of the alloyed silicides was based on the Nb/(Ti + Hf) ratio, which is key regarding creep, the parameters VEC and $\Delta\chi$ and relationships between them. The effect of alloying additions on the stability of "conventional", CC or HE silicide was discussed. The creep and hardness of alloyed Nb_5Si_3 was considered. Relationships that link "conventional", CC or HE bcc solid solution and Nb_5Si_3 in the alloy design methodology NICE (Niobium Intermetallic Composite Elaboration) were presented. For a given temperature and stress, the steady state creep rate of the alloyed silicide, in which TMs substituted Nb, and Al and B substituted Si, depended on its parameters VEC and $\Delta\chi$ and its Nb/(Ti + Hf) ratio, and increased with decreasing parameter and ratio value, compared with the unalloyed Nb_5Si_3. Types of alloyed Nb_5Si_3 with VEC and $\Delta\chi$ values closest to those of the unalloyed Nb_5Si_3 were identified in maps of alloyed Nb_5Si_3. Good agreement was shown between the calculated hardness and chemical composition of Nb_5Si_3 and experimental results.

Keywords: high entropy alloys; complex concentrated alloys; refractory metal intermetallic composites; high entropy silicides; complex concentrated silicides; Nb silicide based alloys; alloy design

check for updates

Citation: Tsakiropoulos, P. On the Nb_5Si_3 Silicide in Metallic Ultra-High Temperature Materials. *Metals* **2023**, *13*, 1023. https://doi.org/10.3390/met13061023

Academic Editor: Sundeep Mukherjee

Received: 20 April 2023
Revised: 18 May 2023
Accepted: 23 May 2023
Published: 26 May 2023

Copyright: © 2023 by the author. Licensee MDPI, Basel, Switzerland. This article is an open access article distributed under the terms and conditions of the Creative Commons Attribution (CC BY) license (https://creativecommons.org/licenses/by/4.0/).

1. Introduction

Metallic ultra-high temperature materials (UHTMs) could replace Ni-based superalloys in high-pressure turbines (HPT) if they could meet property goals for fracture toughness, creep and oxidation or offer a balance of properties [1,2]. Metallic UHTMs currently under development are refractory metal (RM) intermetallic composites (ICs) (i.e., RMICs), RM high entropy alloys (RHEAs) and RM complex concentrated alloys (RCCAs) [1,3–7] (see Appendix A for abbreviations). Like the Ni-based superalloys, in an HPT the new metallic UHTMs will be part of a material system that consists of a metallic UHTM substrate plus environmental coating, most likely of the bond coat/thermally grown oxide/top coat type [2,8–19]. A route to selecting substrate alloys and bond coat alloys for environmental coatings for metallic UHTMs was discussed in [2] and the design of bond coat alloys that form the α-Al_2O_3 scale was discussed in [15,16].

The aforementioned metallic UHTMs can be single-phase or multiphase materials. The RMICs are multiphase materials with microstructures that consist of bcc solid solution(s) and intermetallic(s) [1,2,20–28], whereas the RHEAs and RCCAs can be single-phase bcc solid solution alloys or multiphase alloys with microstructures that consist of solid

solution(s) and intermetallic(s), e.g., [3], or only intermetallics, e.g., [15,16]. For the said categories of metallic UHTMs, the M_5Si_3 silicides (M = transition metal (TM), RM), in particular the Nb_5Si_3 and Mo_5Si_3 silicides, have attracted the interest of alloy designers and developers [1,3,13,24] owing to their creep properties and high Si content that benefits oxidation resistance [29–40]. Other intermetallics that can improve the properties of these three categories of metallic UHTMs are M_3Si silicides, Laves phases and A15 compounds, as well as the $MoSi_2$ and $NbSi_2$ disilicides [1,3,24,41–46]. Eutectics and lamellar microstructures that consist of bcc solid solution and intermetallics also can be present in the microstructures of metallic UHTMs [46–54], for example, see the Table 11 in [51]. The reader who is interested to know why other intermetallics in addition to M_5Si_3 are included in the microstructures of metallic UHTMs could consult [1,24,27,30,42,46].

In the microstructure of multiphase metallic UHTMs, the aforementioned phases can be "conventional" and/or "high entropy" (HE) or "complex concentrated" ("compositionally complex"), i.e., CC. The "conventional", HE and/or CC phases can co-exist in as cast (AC) and/or heat-treated (HT) alloys [24,50–58]. This has been demonstrated for RMICs based on Nb (i.e., RM(Nb)ICs), some of which also are RHEAs or RCCAs (i.e., RM(Nb)ICs/RCCAs or RM(Nb)ICs/RHEAs, see Appendix A) because they meet the definition of the latter two categories of metallic UHTMs [2,7,50,51,56]. Indeed, HEAs and HE phases are those alloys and phases where the maximum and minimum concentrations of elements are not above or below, respectively 35 and 5 at.%, whereas RCCAs alloys and CC phases are those where the maximum and minimum concentrations of elements are above 35 at.% (up to about 40 at.%) and below 5 at.% [1,3,27].

RMICs based on Nb (i.e., RM(Nb)ICs) also are referred to as Nb silicide-based composites or Nb silicide-based in situ composites because in these metallic UHTMs, the alloyed Nb_5Si_3 is formed in situ [1,31,59]. The volume fraction and spatial and size distributions of the aforementioned silicide is key for achieving a balance of properties or meeting a property goal in RM(Nb)ICs, see [1,24,40]. The interested reader can find a detailed background on Nb_5Si_3 silicides and their use in metallic UHTMs in [1,24,27,40].

All three categories of metallic UHTMs with Nb and Si plus other TMs, RMs and simple metal and metalloid element additions can be designed using the alloy design methodology NICE (Niobium Intermetallic Composite Elaboration) [24]. The "engine room" in NICE consists of the parameters ΔH_{mix}, ΔS_{mix}, δ, $\Delta\chi$, VEC and Ω, which are the same parameters that are used to study HEAs [60], and relationships between these parameters and properties of alloys and phases. In NICE, the linking of the alloying behaviour and properties of phases with the said parameters forms the infrastructure that determines/supports the superstructure of metallic UHTMs that can be B free or B containing, Ti free or Ti containing and can have different Ti/Si or Nb/(Ti + Hf) ratios. The reader who is interested to know why B and Ti additions and the Ti/Si and Nb/(Ti + Hf) ratios are important could consult [1,2,24,61,62]. Metallic UHTMs are designed with NICE to meet individual property goals or to offer a balance of properties [1,2,24,56,61,62].

The Nb_5Si_3 that forms in metallic UHTMs can be "conventional" or CC [51] depending on its chemical composition (see above) and can co-exist with "conventional" or CC or HE bcc Nb_{ss} [56] or other CC or HE intermetallics (e.g., see the Table 11 in [51]). In the Nb_5Si_3, TMs and RMs substitute Nb (e.g., Cr, Fe, Hf, Mo, Ta, Ti, V, W and Zr) and simple metals and metalloid elements substitute Si (e.g., Al, B, Ge and Sn) [40]. Research has confirmed that the aforementioned alloying elements in metallic UHTMs are key for improving important properties, namely yield strength, creep and oxidation resistance, for example, see [1,3,5–9,17,20–22,24,26,36,42,50,52–54,57–59,61,62]. Simultaneous use of the aforesaid solutes is not essential, the alloy design methodology NICE can guide the alloy designer regarding the choice of alloying additions and their concentrations in a metallic UHTM, for example, see [2,15–17,24,27,62].

The alloyed Nb_5Si_3 silicide can be "normal" and/or Ti and Hf rich in the AC and HT alloy according to the partitioning of solutes [24,40] (also the bcc solid solution can be "normal" or Ti rich or Si free, according to the partitioning of solutes [1,24,55]), can have

high or low Nb/Ti or Nb/(Ti + Hf) ratios [40], its crystal structure can be tetragonal or hexagonal depending on alloying additions and interstitial contamination [40,51,63–67]. For B-free RM(Nb)ICs, the Nb/(Ti + Hf) ratio is important for (i) the creep properties of the alloy (the ratio must be higher than 1.4) [35], (ii) the crystal structure of the silicide [68] and (iii) the design of bond coat alloy(s) for an environmental coating [16].

Since the classification of new alloys as HEAs or CCAs, excellent mechanical properties have been reported for some of the single-phase solid solution materials [60]. Similarly, outstanding mechanical properties (e.g., yield strength) have been reported for some RCCAs and RHEAs [3] and for multiphase RMICs [1,2,27], with properties (e.g., specific strength and oxidation resistance) of some of the latter alloys and properties (e.g., hardness) of their bcc solid solutions greater than those of the former alloys [1,27,56,61,62,67]. In addition, the creep of some RMICs is close to the creep property goal for metallic UHTMs [1]. Furthermore, some RMICs have outstanding (for RM alloys) oxidation in the pest temperature range and simultaneously at high temperatures, e.g., see [27,62,65], which, to the author's knowledge, currently is not the case for RCCAs and RHEAs [3].

In RMICs, the key phases, namely bcc solid solution and 5–3 silicide [24,27,40,44,49], can be "conventional", CC or HE, see above and [51,56]. Recently, the stability of CC or HE Nb_{ss} in RM(Nb)ICs, RM(Nb)ICs/RCCAs and RM(Nb)ICs/RHEAs was studied in [56]. A similar study for the Nb_5Si_3 silicide is missing. This paper aspires to address this oversight. In particular, some key questions regarding the Nb_5Si_3 in metallic UHTMs, which are important for the design of these materials, will be considered. In RM(Nb)ICs, RM(Nb)ICs/RCCAs and RM(Nb)ICs/RHEAs the type of stable Nb_5Si_3, meaning "conventional", CC or HE, is determined by (dependent on) alloying additions. Are there relationships between (a) the parameters (i) of the alloyed Nb_5Si_3 (ii) of alloy and alloyed Nb_5Si_3 (iii) of silicide and bcc solid solution and (b) the parameters and the Nb/(Ti + Hf) ratio of the silicide? How do alloying additions affect the creep of alloyed Nb_5Si_3? Can the alloy developer select alloying elements and type of Nb_5Si_3 (meaning "conventional", CC or HE) that are desirable for the "best" creep properties of the silicide?

In this paper, I shall deliberate on the type of Nb_5Si_3 ("conventional" or CC/HE) in different groups of alloys to consider, for the first time, the effect of specific alloying additions, whether TMs, RMs or simple metal and metalloid element in $(Nb, Ti, Cr)_5(Si, Al)_3$ and discuss the hardness of the silicide. With guidance from NICE, relationships between parameters, and parameters and solutes will be sought and the effect of alloying additions on the creep of Nb_5Si_3 will be discussed. I shall classify Nb_5Si_3 silicides as "conventional" or CC/HE, using published data about the chemical composition of Nb_5Si_3 silicides in RMICs, and with this data I shall also present, for the first time, the relationships between parameters and discuss the importance of the Nb/Ti and Nb/(Ti + Hf) ratio of the silicide. Moreover, I shall suggest creep experiments on tetragonal Nb_5Si_3 with specific alloying elements substituting Si or Nb and Si, which in my opinion are essential to understand better how alloying affects the creep of Nb_5Si_3.

HE or CC ceramics and silicides have been studied as single-phase materials, e.g., [69–72]. Single-phase materials are not considered in this paper. Scarce data about the chemical composition of phases in multiphase RHEAs or RCCAs with Nb and Si addition shows that their phases can be "conventional", CC or HE, for example, see (i) the RHEA alloy $NbCrMoTiVAl_{0.5}Si_{0.3}$ in [52] where the solid solution is CC, the Nb_5Si_3 is HE and the eutectic of these two phases is also HE and (ii) the RHEA alloy $Mo_{0.5}NbHf_{0.5}ZrTiSi_x$ in [53] where the eutectic is HE. The aforementioned RHEAs in the references [52,53] in which they were referred to as high entropy composite and refractory high entropy $(Mo_{0.5}NbHf_{0.5}ZrTi)_{BCC}/M_5Si_3$ in situ compound, respectively, and classified as RHEAs in [3], strictly speaking, are refractory metal high entropy intermetallic composites (i.e., RMICs/RHEAs).

There are no systematic studies of M_5Si_3 silicides in RHEAs or RCCAs that would allow one to answer the questions asked above for alloyed 5–3 silicides in these metallic UHTMs, in particular the dependence of the type of alloyed Nb_5Si_3 on alloying additions, and how alloying additions affect the creep of alloyed Nb_5Si_3. Thus, owing to the lack

of such studies of alloyed Nb_5Si_3 silicides in multiphase RCCAs or RHEAs, the focus of this paper will be alloyed Nb_5Si_3 silicides only in RM(Nb)ICs, RM(Nb)ICs/RCCAs or RM(Nb)ICs/RHEAs that have been studied systematically in our research group and which can be arranged in different groups/sets depending on the "basis" alloy. The chemical compositions of the alloys are given in Appendix B, where also are given references where the interested reader can find the experimental data about the structure and chemical analysis of alloyed Nb_5Si_3 silicides. In this paper, the alloys are arranged in four groups/sets, as discussed in the next section, in order to show the effect of alloying, meaning the substitution of Nb or Si by specific solutes, on the type of Nb_5Si_3 silicide.

2. Complex Concentrated Nb_5Si_3

RM(Nb)ICs, RHEAs and RCCAs not only use the same alloying elements [1,2,27] and their phases can be displayed in the same $\Delta\chi$ versus VEC map [2], but also can be presented together in the same $\Delta\chi$ versus δ map [1,2,73]. In the latter map, the alloys with B addition are found in a distinctly different location from KZ series alloys with/without RM and simple metal and metalloid element additions [73] (KZ series alloys are based on Nb-24Ti-18Si (at.%, nominal) with the addition of Al and/or Cr (each at 5 at.%, nominal)).

To study the effects of specific alloying additions on the type (meaning "conventional", CC/HE) and stability of Nb_5Si_3, I shall (i) make use of maps in which (a) alloys will be grouped together using a different "basis" alloy and (b) different colours will be employed for different alloy conditions, namely dark colours for the AC condition and light colours for the HT condition, (ii) use blue colour for "normal" Nb_5Si_3 and red colour for Ti rich Nb_5Si_3 and (iii) give (only for presentation purposes to enable comparison of silicides in different alloys) the "values" 15 and 10, respectively for "conventional" Nb_5Si_3 and CC Nb_5Si_3 to schematically distinguish (separate) the two silicides, see Figures 1–4. Note that in this paper, the Nb_5Si_3 silicide is studied in alloys in which the bcc solid solution Nb_{ss} recently was studied as "conventional", CC or HE, see [56], i.e., in alloys where "conventional", CC/HE Nb_{ss} and Nb_5Si_3 co-exist. It will be shown that there exist relationships between Nb_{ss} and Nb_5Si_3, in addition to relationships between parameters of Nb_5Si_3. For the calculation of the parameters VEC and $\Delta\chi$ of the silicide, the reader should refer to [40].

The "normal" Nb_5Si_3 of an alloy can be "conventional" or CC in both the AC and HT conditions, in which case, its *y*-axis "value" in Figures 1a, 2a, 3a and 4a will be 15 or 10, respectively, and the silicide will be shown with dark blue colour in the AC condition and light blue colour in the HT condition. Alternatively, the silicide could be Ti rich and "conventional" or CC in the AC and HT conditions, in which case its *y*-axis "value" would be 15 or 10, respectively, and the Ti-rich Nb_5Si_3 will be shown with dark red colour in the AC condition and light pink colour in the HT condition.

In the first group/set of Nb_5Si_3, shown in Figure 1a, the basis alloy is the alloy KZ5 and the group is made up of silicides in the RM(Nb)ICs KZ5, KZ6, JG2, JG3, JN1, TT4, ZF6 and ZX8 (see the Appendix B for the nominal alloy compositions and references, note that the chemical analysis data was obtained using EPMA or EDS with standards). These alloys were chosen to show the effect of the addition of B, Ge, Hf, Mo, Sn or Ta to KZ5 (the basis alloy) on the type ("conventional" or CC) of Nb_5Si_3 or, in other words, to show the effect of the synergy of Al, Cr and Ti in $(Nb, Ti and Cr)_5(Si and Al)_3$ (i.e., the 5–3 silicide in the basis alloy, where Nb is substituted with Cr and Ti, and Si with Al) with B, Ge, Hf, Mo, Sn or Ta (the specific alloying addition) in the silicide in the aforementioned RM(Nb)ICs. In Figure 1a each solute addition to the basis alloy is indicated in parenthesis.

In the basis alloy KZ5, the "normal" Nb_5Si_3 and Ti-rich Nb_5Si_3 (dark blue and red colours—AC condition) was "conventional" (the *y*-axis "value" is 15) in both the AC and HT (lighter blue and pink colours) conditions. With each addition to the basis alloy, the Ti rich Nb_5Si_3 became CC (the *y*-axis "value" is 10). With the addition of Ge, Hf or Sn, the status (rank) of the "normal" silicide as "conventional" did not change. With the addition of B, the Ti rich Nb_5Si_3 was not stable after HT. The Mo addition in the alloys JG2 and JG3 (note the lower Mo content in JG3, see the Appendix B) showed that the Mo concentration

in the alloy is important regarding the promotion or not of CC Nb_5Si_3. The addition of Ta was more effective regarding the formation of CC Nb_5Si_3 in the AC alloy compared with the addition of Mo when the latter was at low concentration, otherwise Mo and Ta were equally effective at high (about 5 to 6 at.%) concentrations in the alloy.

The partitioning of Ti to Nb_5Si_3 affects the Nb/Ti or Nb(Ti + Hf) ratio of the "conventional" and CC silicide (Figure 1b). The effect depends on alloying addition, for example, it was severe for the Ti-rich Nb_5Si_3 (CC silicide) with the addition of Hf in the alloy (compare the silicide in the alloys KZ5 and JN1). Compared with the AC condition, in the HT condition, the said ratio of the Ti-rich Nb_5Si_3 (CC silicide) was lower and higher when Mo or Hf and Ge or Ta, respectively, were added to the basis alloy (compare the silicide in the alloys JN1 and JG3, and the alloys ZF6 and KZ6). Only with the addition of Sn the said ratio of the "conventional" Nb_5Si_3 increased in the HT condition (alloy ZX8). Furthermore, the Nb/(Ti + Hf) ratio of the Ti-rich silicide (CC Nb_5Si_3) in the alloy JN1 was less than one (hexagonal silicide [68]).

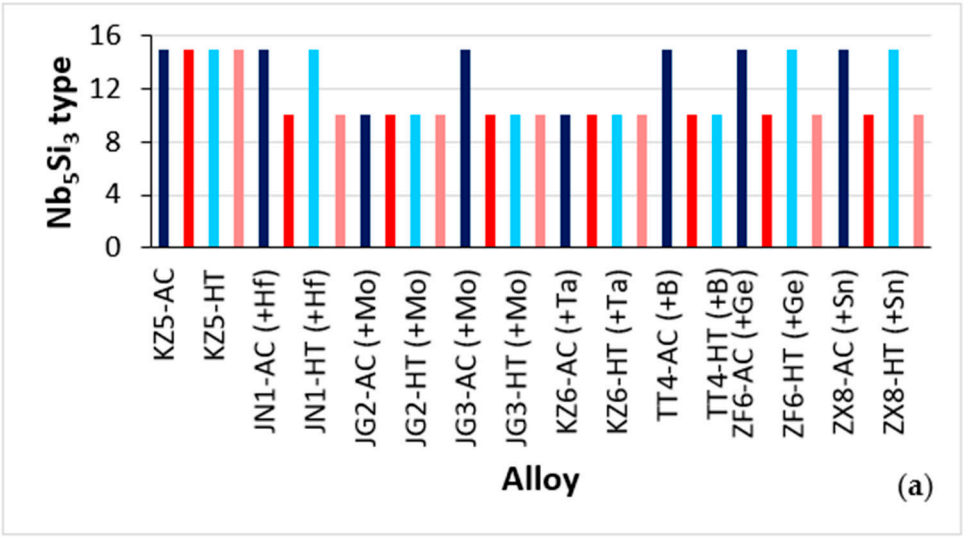
The alloying additions to the basis alloy also affect the parameters VEC and $\Delta\chi$ of the Nb_5Si_3, see Figure 1c,d. Compared with the basis alloy KZ5, the changes of the parameters VEC and $\Delta\chi$ were more severe, respectively with the addition of Hf (Figure 1c, silicide in alloy JN1) and B or Ta (Figure 1d, silicide in the alloys TT4 and KZ6). Compared with the AC condition, in the HT condition, the parameter VEC of the Ti-rich Nb_5Si_3 (CC silicide) decreased and increased, respectively with the addition of Hf or Mo and Ge or Ta (Figure 1c, silicide in the alloys JN1, JG2 and JG3 and the alloys ZF6 and KZ6). With the exception of the B addition in the alloy TT4, the value of the parameter VEC of the "conventional" "normal" Nb_5Si_3 exceeded 4.4. In the alloy TT4, the Ti-rich Nb_5Si_3 (CC Nb_5Si_3) had the lowest VEC (about 4.27).

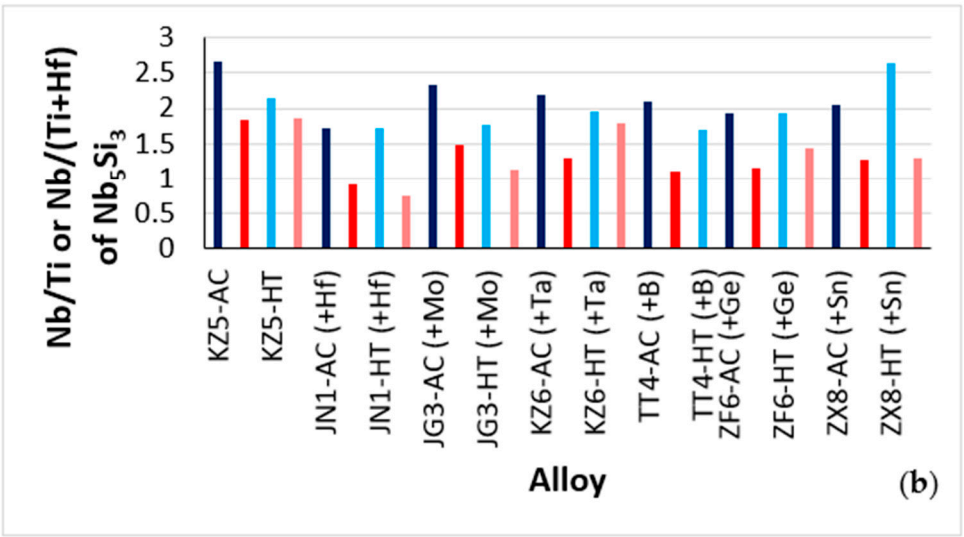
The parameter $\Delta\chi$ of the "conventional" Nb_5Si_3 decreased in the HT condition compared with the AC condition in the basis alloy and with the addition of Ge, Hf, 5 at.% Mo, Sn or Ta, but increased when the concentration of Mo was decreased to 2 at.% (Figure 1d, silicide in the alloys KZ5, JN1, JG2, KZ6, ZX8, ZF6 and the alloy JG3). In contrast, the parameter $\Delta\chi$ of the CC Nb_5Si_3 increased in the HT condition compared with the AC condition in the basis alloy and with the addition of Ge (Figure 1d, silicide in the alloys KZ5 and ZF6), and decreased with the addition of B, Hf, Mo, Sn or Ta (silicide in the alloys TT4, JN1, JG2, JG3, ZX8, KZ6). Note that the change of the Mo concentration in the alloy affected only the parameter $\Delta\chi$ of the "conventional" silicide. Moreover, note that the lowest and highest $\Delta\chi$ values for "conventional" and CC Nb_5Si_3 were with the addition of B and Ge (silicide in the alloys TT4 and ZF6).

The trends of the VEC versus $\Delta\chi$ data of the Nb_5Si_3 for the addition of B, Ge, Hf, Mo, Sn or Ta to the basis alloy KZ5 are shown in the map in Figure 1e. Note (i) similar trends for the addition of Ge or Sn, Ta or B and Hf or Mo, (ii) that with the addition of B or Ta, the parameter $\Delta\chi$ is less than about 0.31, whereas with the addition of Hf, Mo or Sn, the $\Delta\chi$ was higher and in the range 0.3 to 0.41, (iii) the narrow $\Delta\chi$ range with the addition of Ge, (iv) maxima with the addition of B (0.2546, 4.338), Hf (0.3757, 4.429), Mo (0.3589, 4.435) or Ta (0.2676, 4.421) and (v) minima with the addition of Ge (0.4038, 4.294) and Sn (0.3618, 4.356), where in parenthesis is given the corresponding $\Delta\chi$ and VEC of maximum or minimum. The relationship between the Nb/Ti or Nb/(Ti + Hf) ratio and the parameter VEC of Nb_5Si_3 is shown in Figure 1f. High ratio values link with high VEC values of the silicide.

In the second group/set of Nb_5Si_3, shown in Figure 2a, the basis alloy is the alloy JN1 (i.e., KZ5 + Hf) and the group is made up of the alloys JN1, JG4, TT7, ZF9 and EZ8 (see the Appendix B for the nominal alloy compositions and references). These alloys were chosen to show the effect of the synergy of Hf with the addition of B, Ge, Mo or Sn on the type ("conventional" or CC) of Nb_5Si_3 or, in other words, to show the effect of the synergy of Al, Cr, Hf and Ti in $(Nb, Ti, Cr, Hf)_5(Si, Al)_3$ (note this is different from the $(Nb, Ti, Cr)_5(Si, Al)_3$ of the first group/set owing to substitution of Nb with Hf, as well as with Cr and Ti) in the basis alloy with the addition of B, Ge, Mo or Sn (the specific alloying addition) in the aforementioned RM(Nb)ICs and RM(Nb)ICs/RCCAs. In Figure 2a, each solute addition to

the basis alloy is indicated in parenthesis. Note that in this group the alloys EZ8, TT7 and ZF9 are RM(Nb)ICs/RCCAs.





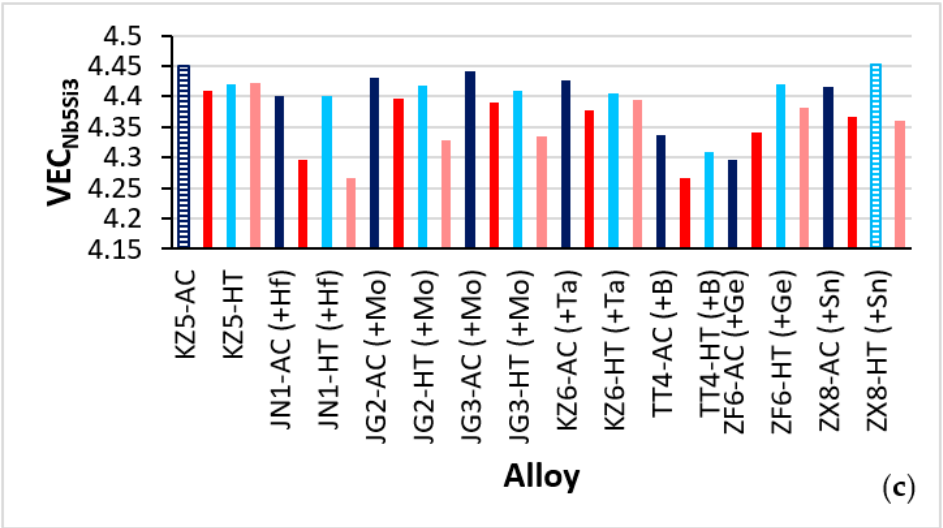
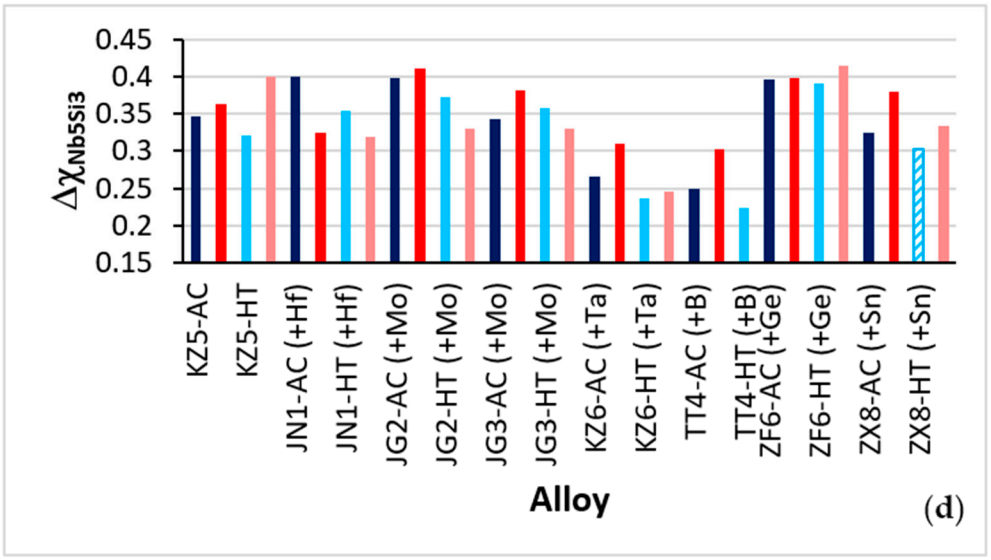
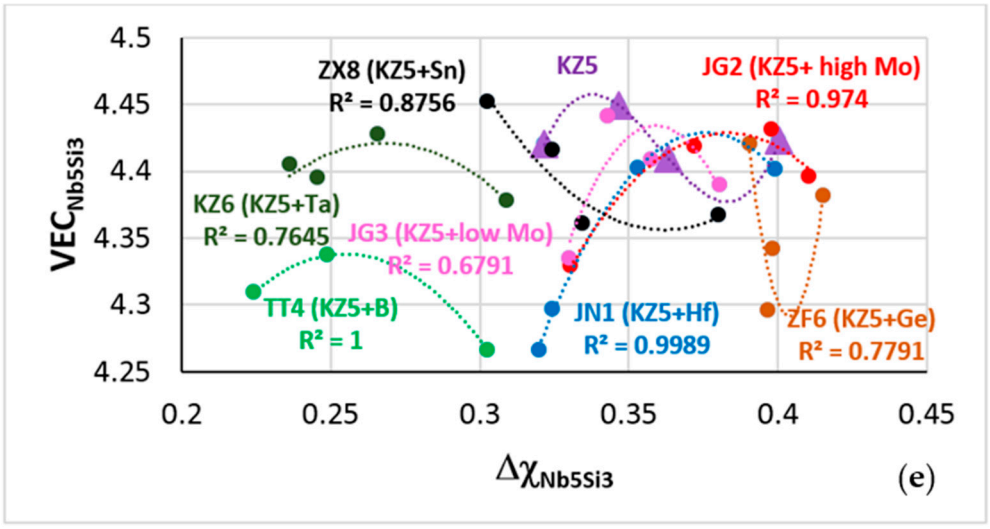


Figure 1. *Cont.*





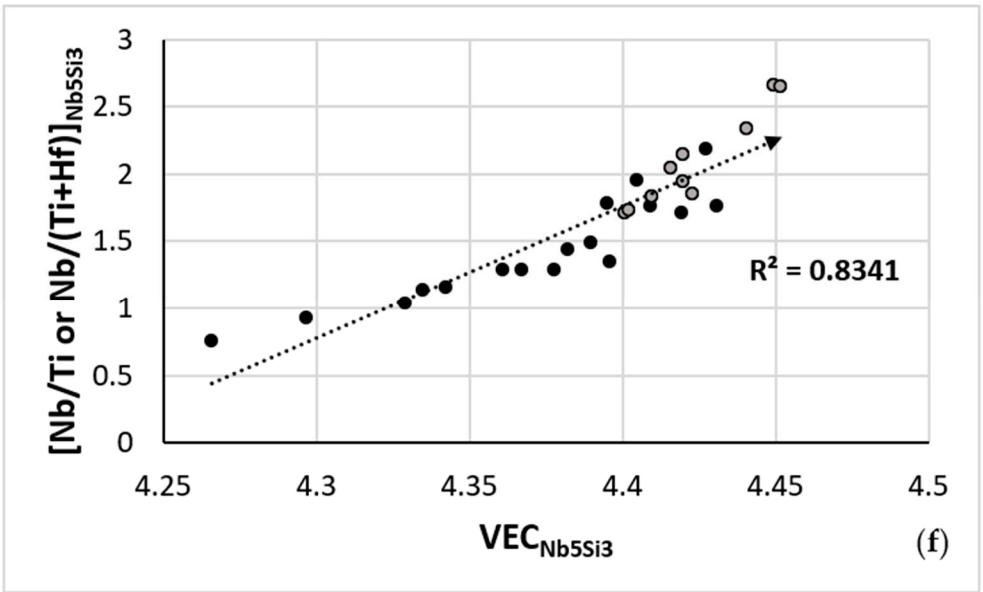


Figure 1. *Cont.*

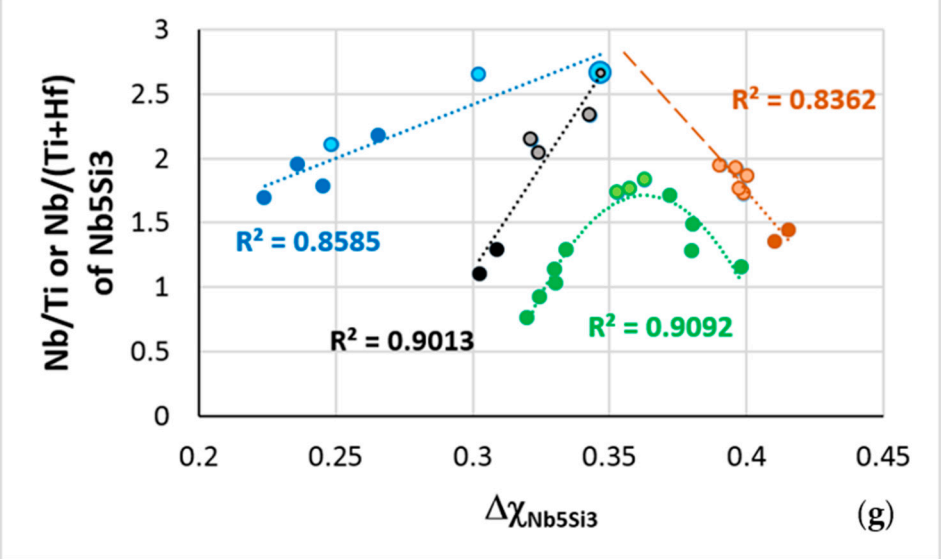
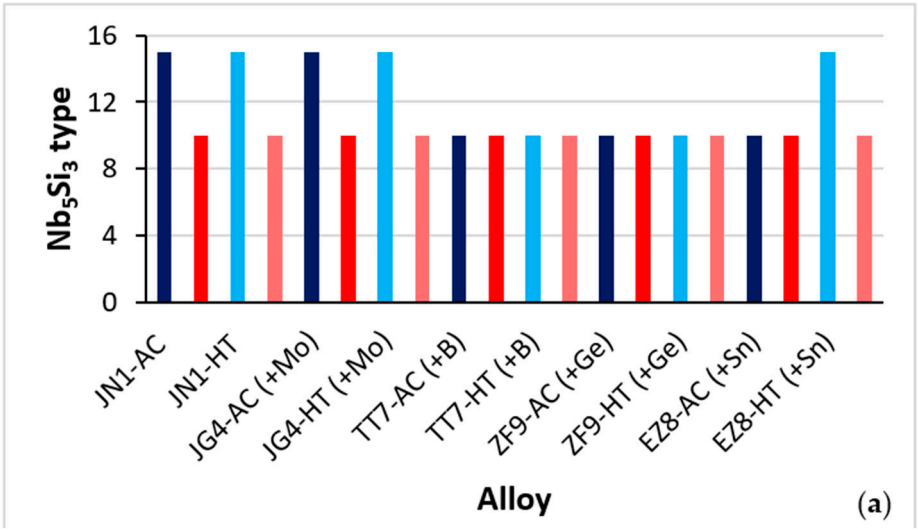


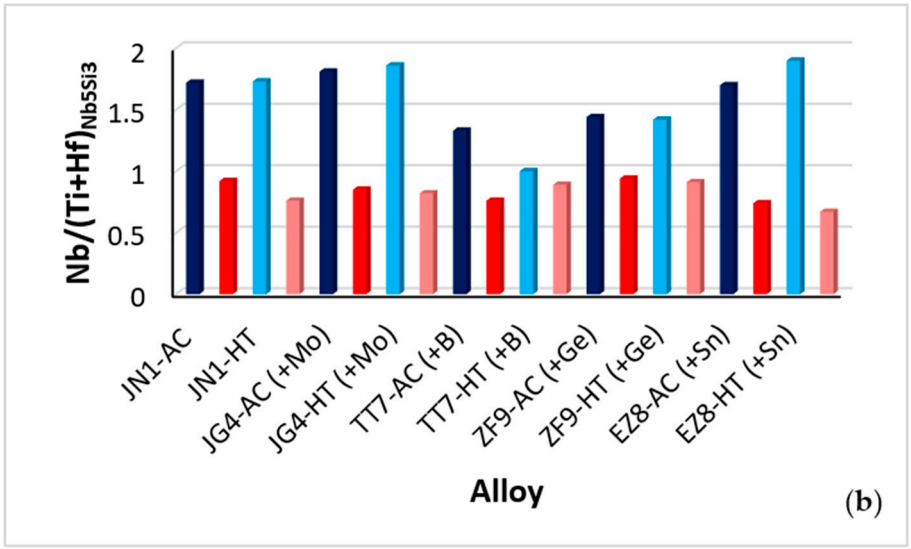
Figure 1. Data for Nb_5Si_3 in RM(Nb)ICs with basis alloy KZ5 (Nb-24Ti-18Si-5Al-5Cr, at.%, nominal) and alloying additions B, Ge, Hf, Mo, Sn or Ta (shown in parentheses in (**a**,**d**)). Alloys KZ5, KZ6, JG2, JG3, JN1, TT4, ZF6 and ZX8. For nominal alloy compositions and references, see the Appendix B. (**a**) Type of Nb_5Si_3 ("conventional" or CC), dark and lighter colours, respectively for AC and HT conditions. For presentation purposes, the "values" 15 and 10 have been assigned, respectively to "conventional" Nb_5Si_3 and CC Nb_5Si_3. (**b**) Nb/Ti or Nb/(Ti + Hf) ratio of Nb_5Si_3, (**c**) VEC of Nb_5Si_3, (**d**) $\Delta\chi$ of Nb_5Si_3, (**e**) VEC versus $\Delta\chi$ of Nb_5Si_3 and (**f**) Nb/Ti or Nb/(Ti + Hf) ratio versus VEC of Nb_5Si_3. See text for hatched data in (**c**,**d**) and for the arrow in (**f**). In (**d**,**e**), the parameter $\Delta\chi$ is based on the Pauling electronegativity. In (**f**), the light colour data is for "conventional" silicide. In (**e**), JZ2 = KZ5 + 5 Mo and JG3 = KZ5 + 2 Mo (at.%). (**g**) Nb/(Ti + Hf) versus $\Delta\chi$ of Nb_5Si_3. In (**g**), lighter colours indicate "conventional" Nb_5Si_3 and darker colours CC Nb_5Si_3, parabolic fit of green data gave $R^2 = 0.9092$, all other R^2 values are for linear fit of data. In (**g**), blue data is for the alloys KZ5, KZ6, TT4, ZX8, black data for the alloys KZ5, KZ6, TT4, ZX8 plus JG3, green data for the alloys KZ5, JG2, JG3, JN1, ZF6, ZX8 and brown data for the alloys KZ5, JG2, JN1, ZF6, i.e., no B, Sn or Ta additions in brown data, no B or Ta in green data, no Ge or Hf in black data and no Ge, Hf or Mo in blue data.

In the basis alloy JN1, the "normal" Nb_5Si_3 and Ti-rich Nb_5Si_3 (dark blue and red colours-AC condition), respectively "conventional" and CC (the *y*-axis "values", respectively are 15 and 10) in both the AC and HT (lighter blue and pink colours) conditions. The "status" (rank) of the silicide did not change with the addition of 2 at.% Mo (alloy JG4), but with the addition of B or Ge the "normal" and Ti-rich Nb_5Si_3 were CC in both the AC and HT conditions (silicide in the alloys TT7 and ZF9), whereas with the addition of Sn the CC Nb_5Si_3 in the alloy, EZ8-AC changed to "conventional" silicide after the heat treatment (Figure 2a). With all solute additions to the basis alloy, the "status" (rank) of the Ti-rich Nb_5Si_3 did not change, i.e., it was CC. The synergy of Hf with the low concentration of Mo (alloy JG4) was less effective than the synergy of B with Hf regarding the conversion of the "conventional" Nb_5Si_3 to CC. For the former synergy, this effect was attributed to Hf for the latter was attributed to B (compare with Figure 1a). Furthermore, the synergy of Ge and Hf was more effective than the synergy of Hf and Sn regarding the conversion of the "conventional" Nb_5Si_3 to CC (compare with Figure 1a).

The Nb/(Ti + Hf) ratio of the "conventional" silicide increased in the HT condition in the basis alloy and with the addition of Ge, Mo or Sn (Figure 2b), and was higher than 1.5 (tetragonal silicide [68]) in the basis alloy JN1 and with the addition of Mo or Sn. However, this ratio was lower than one (indicative of hexagonal structure [68]) for the Ti rich Nb_5Si_3 (CC) in the basis alloy, and with the addition of B, Ge, Mo or Sn in the alloys TT4, ZF6, JG4 and ZX8. Furthermore, the Nb/(Ti + Hf) ratio of the Nb_5Si_3 alloyed with Hf and B, Ge, Mo

or Sn did not exceed 1.9, and was lower than that of the silicide in the alloys with KZ5 as their basis (compare Figures 1b and 2b).





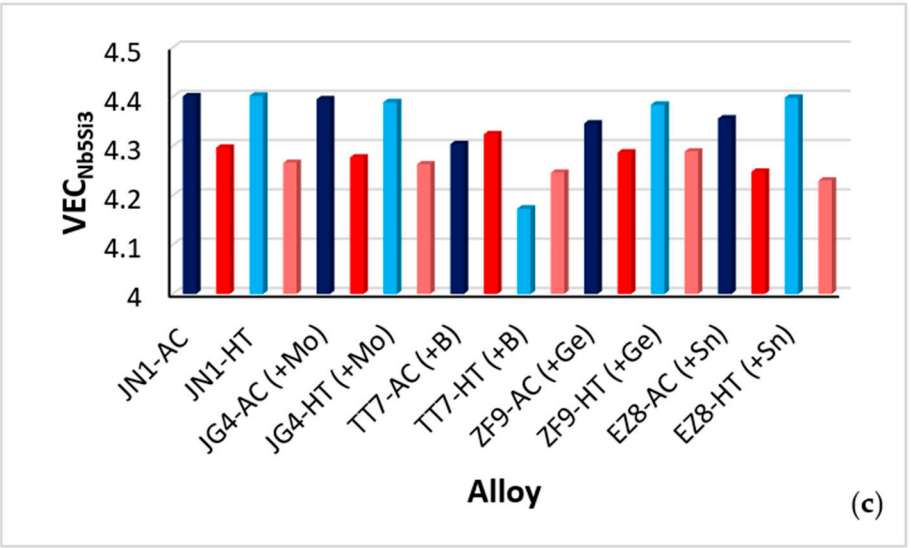


Figure 2. *Cont.*

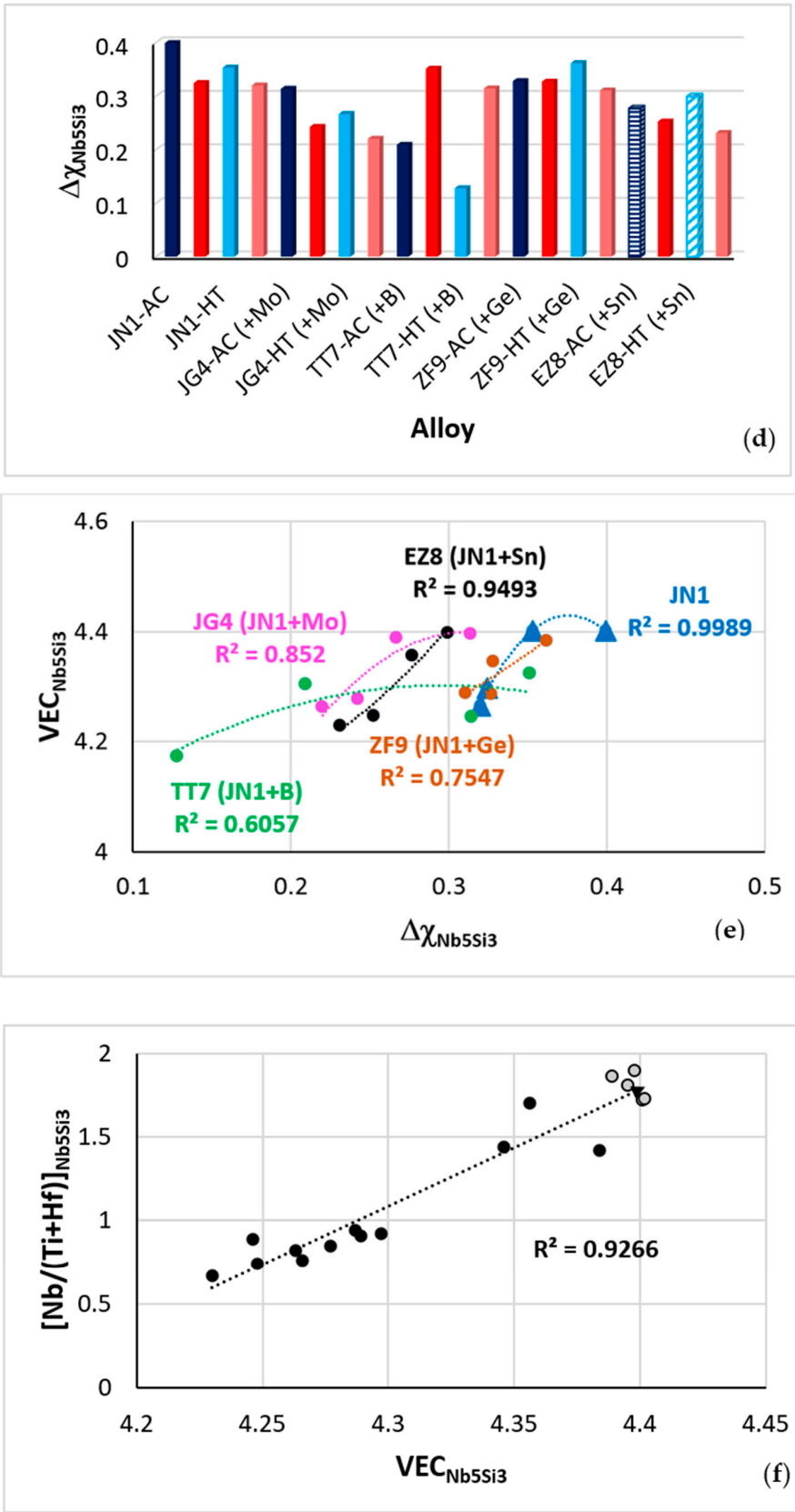


Figure 2. Data for Nb_5Si_3 in RM(Nb)ICs and RM(Nb)ICs/RCCAs with basis alloy JN1 (Nb-24Ti-18Si-5Al-5Cr-5Hf, at.%, nominal) and alloying additions B, Ge, Mo or Sn (shown in parenthesis). Alloys JN1, JG4, TT7, ZF9 and EZ8. For nominal alloy compositions and references, see the Appendix B. (**a**) Type of Nb_5Si_3 ("conventional" or CC), dark and lighter colours, respectively for AC and HT

conditions. For presentation purposes, the "values" 15 and 10 have been assigned, respectively to "conventional" Nb_5Si_3 and CC Nb_5Si_3. (**b**) Nb/(Ti + Hf) ratio of Nb_5Si_3, (**c**) VEC of Nb_5Si_3, (**d**) $\Delta\chi$ of Nb_5Si_3, (**e**) VEC versus $\Delta\chi$ of Nb_5Si_3 and (**f**) Nb/(Ti + Hf) ratio versus VEC of Nb_5Si_3. In (**d**,**e**), the parameter $\Delta\chi$ is based on the Pauling electronegativity. See text for hatched data in (**d**) and for the arrow in (**f**). In (**f**), the light colour data is for "conventional" silicide. In (**e**), the R^2 values are for parabolic fit of data. RM(Nb)ICs/RCCAs the alloys EZ8, TT7 and ZF9.

The highest VEC values (about 4.4) were for the "conventional" silicide of the basis alloy in the AC and HT conditions and after the addition of Mo (alloy JG4), and in the alloy EZ8-HT (addition of Sn), Figure 2c. These VEC values were lower than the highest VEC values of silicides in the alloys with KZ5 as their basis (compare with Figure 1c). The parameter VEC of the CC Ti rich Nb_5Si_3 decreased after heat treatment, with the exception of the alloy ZF9 (addition of Ge) where it did not change. The lowest VEC value (4.173), which was for the CC Nb_5Si_3 in the alloy TT7-HT (addition of B), was lower than the lowest VEC of the alloys considered in Figure 1.

The parameter $\Delta\chi$ of the silicide decreased with the addition of B, Mo or Sn to the basis alloy JN1, with the exception of the CC Ti rich Nb_5Si_3 in the alloy TT7-AC (B addition) and did not change significantly with the addition of Ge (Figure 2d). Both the lowest $\Delta\chi$ value (0.128), which was for the CC Nb_5Si_3 in the alloy TT7-HT (B addition), and the highest $\Delta\chi$ value (0.4) that was for the "conventional" silicide in the alloy JN1-AC (basis alloy), were lower than the parameter $\Delta\chi$ of the silicide in the alloys considered in Figure 1. In other words, the synergy of Hf with Al, Cr and Ti plus B, Ge, Mo or Sn in Nb_5Si_3 decreased the parameters VEC and $\Delta\chi$ compared with the Hf-free Nb_5Si_3 (the parameter VEC changed from the range 4.452 to 4.266 to the range 4.402 to 4.173 and the parameter $\Delta\chi$ changed from the range 0.415 to 0.224 to the range 0.399 to 0.128).

The map of the parameters VEC and $\Delta\chi$ of the Nb_5Si_3 in the alloys with JN1 as their basis is shown in Figure 2e. Note (i) similar trends for the basis alloy JN1 and for the additions of B (alloy TT7) or Mo (alloy JG4), (ii) similar trends for the additions of Ge (alloy ZF9) or Sn (alloy EZ8), (iii) maxima for the additions of B (0.296, 4.3025) or Mo (0.312, 4.399) and the basis alloy (0.376, 4.429) and (iv) that the B, Ge, Mo or Sn addition reduced the parameters $\Delta\chi$ and VEC. Compared with the Hf free Nb_5Si_3 in the alloys considered in Figure 1, the B and Mo maxima shifted, respectively to higher and lower $\Delta\chi$ and VEC values in the case of B addition, and to both lower $\Delta\chi$ and VEC values in the case of Mo addition. The relationship between the Nb/(Ti + Hf) ratio and the parameter VEC of Nb_5Si_3 is shown in Figure 2f. High ratio values link with high VEC values of the silicide. The figure confirms the lower range of the parameter VEC for the second group of alloys. Note that the slope of the line in Figure 2f is less than that in Figure 1f.

In the third group/set of Nb_5Si_3, shown in Figure 3a, the basis alloy is the alloy TT4 (i.e., KZ5 + B) and the group is made up of the alloys TT4, TT5, TT6, TT7 and TT8 (see the Appendix B for the alloy compositions and references). These alloys were chosen to show the effect of the synergy of B with the Hf, Mo, Sn or Ta additions on the type ("conventional" or CC) of tetragonal T2-$Nb_5(Si, B)_3$ or, in other words, to show the effect of the synergy of Al, Cr, B and Ti in T2-$(Nb, Ti, Cr)_5(Si, Al, B)_3$ (note this is different from $(Nb, Ti, Cr)_5(Si, Al)_3$ of the first group owing to the substitution of Si with B as well as with Al) in the basis alloy with the addition of Hf, Mo, Sn or Ta (the specific alloying addition) in the aforementioned RM(Nb)ICs and RM(Nb)ICs/RCCAs. Each solute addition to the basis alloy is indicated in parenthesis. Note that in this group, the alloys TT5, TT6 and TT7 are RM(Nb)ICs/RCCAs.

In the basis alloy TT4-AC, the "normal" T2 and Ti-rich T2 (dark blue and red colours-AC condition), respectively was "conventional" and CC (the *y*-axis "values", respectively are 15 and 10) and both were CC in the HT (lighter blue and pink colours) condition (Figure 3a). The Mo addition did not promote the conversion of "conventional" T2 to CC after heat treatment, and the Sn addition did not prevent the CC silicide from converting to "conventional" after heat treatment. This behaviour was the same as that observed for the synergies of Hf and Mo and Hf and Sn (compare Figures 2a and 3a). On the contrary, with the additions of Hf or Ta, the CC silicide ("normal" or Ti rich) in the AC alloys was stable

after HT (silicide in the alloys TT5-HT and TT7-HT). In other words, the "conventional" T2 was stable after heat treatment when the silicide was alloyed with Mo or Sn.

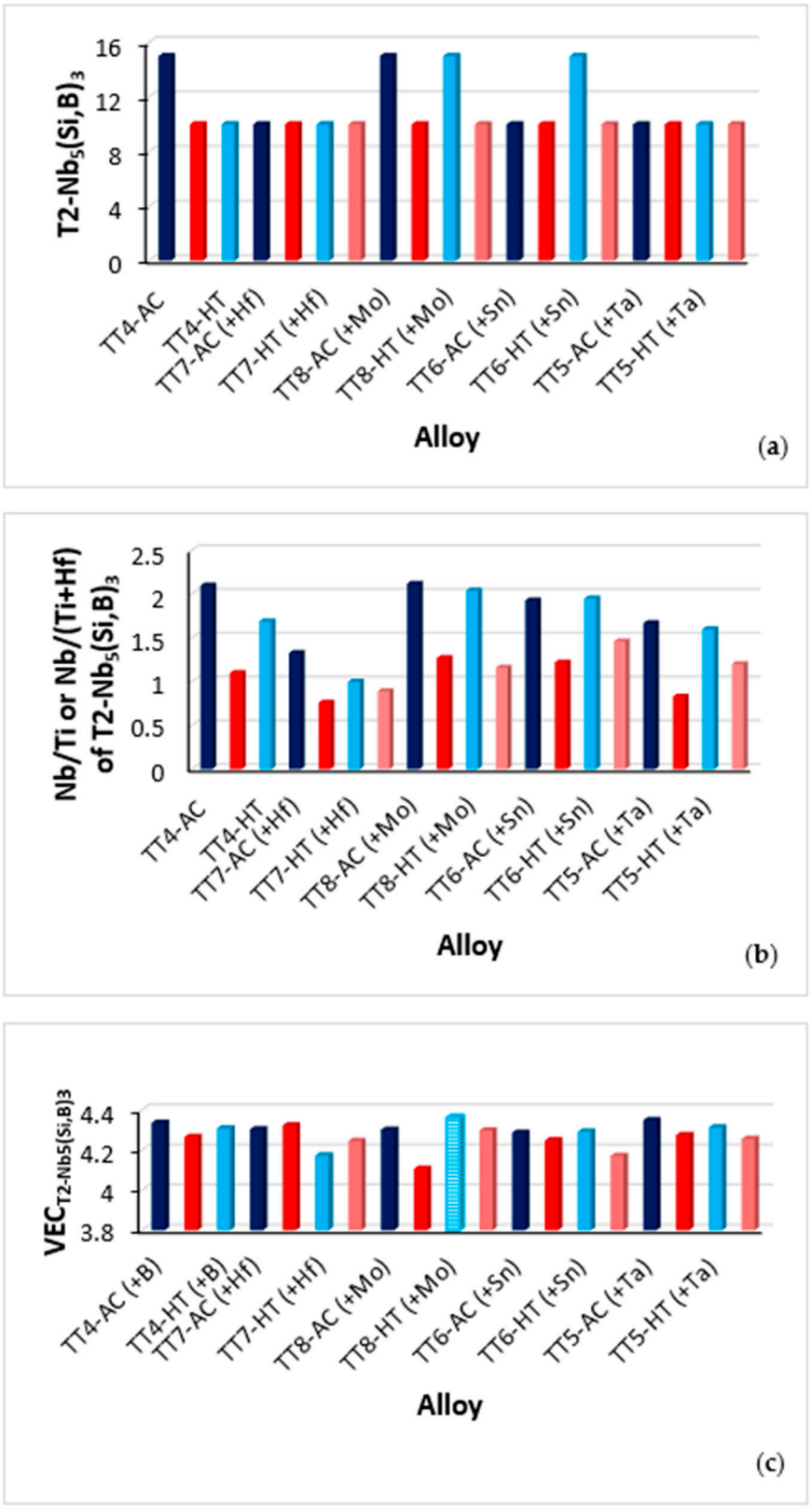


Figure 3. *Cont.*

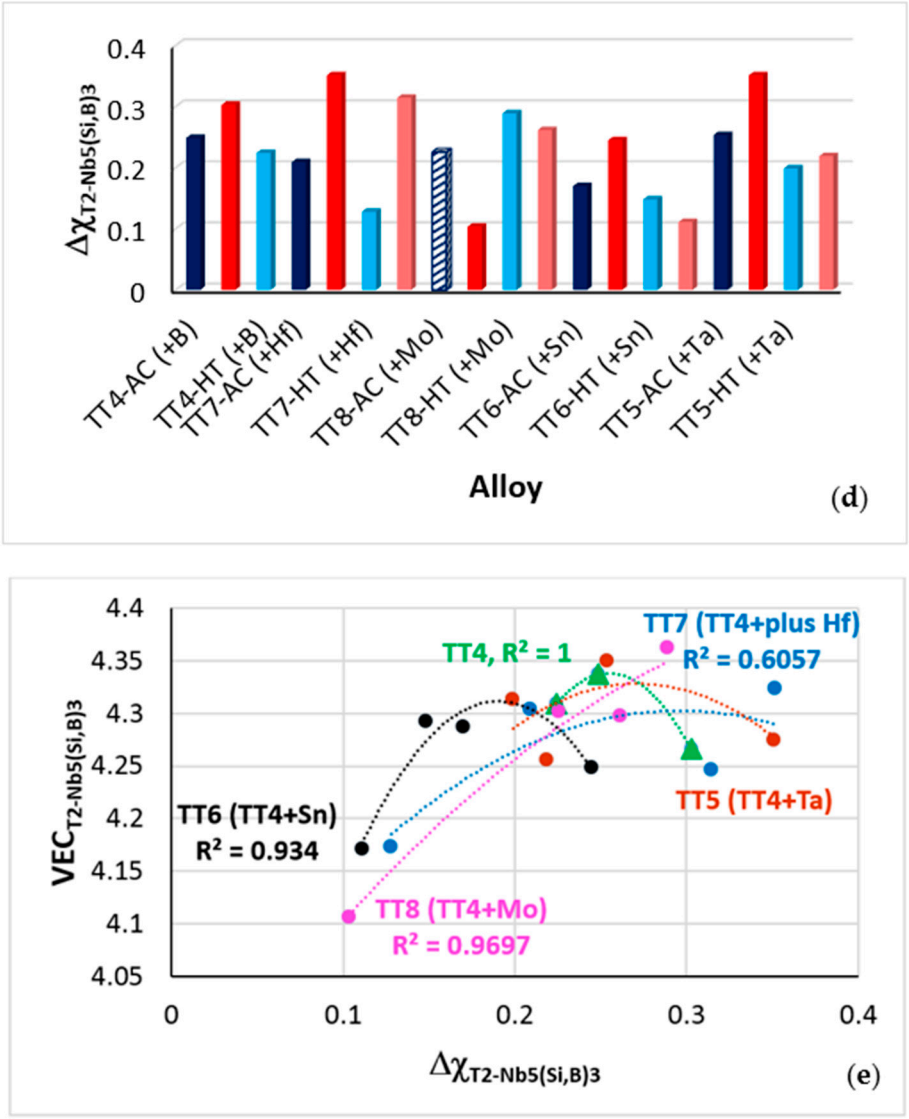


Figure 3. Data for tetragonal T2-$Nb_5(Si, B)_3$ in RM(Nb)ICs and RM(Nb)ICs/RCCAs with basis alloy TT4 (KZ5 + B) and alloying additions Hf, Mo, Sn or Ta (shown in parenthesis). Alloys TT4, TT5, TT6, TT7 and TT8. For nominal alloy compositions and references, see the Appendix B. (**a**) Type of T2 silicide ("conventional" or CC), dark and lighter colours, respectively for the AC and HT conditions. For presentation purposes, the "values" 15 and 10 have been assigned, respectively to "conventional" T2 and CC T2. (**b**) Nb/Ti or Nb/(Ti + Hf) ratio of T2, (**c**) VEC of T2, (**d**) $\Delta\chi$ of T2 and (**e**) VEC versus $\Delta\chi$ of T2. See text for hatched data in (**c**,**d**). In (**d**,**e**), the parameter $\Delta\chi$ is based on the Pauling electronegativity. In (**e**), the R^2 values are for the parabolic fit of data. Poor fit of data for the Ta addition. RM(Nb)ICs/RCCAs are the alloys TT5, TT6 and TT7.

For the "conventional" T2 silicide, the synergy of B with Mo in the AC and HT alloy TT8 resulted in a similar Nb/Ti ratio with the basis alloy TT4-AC (Figure 3b). The Nb/Ti and Nb/(Ti + Hf) ratio of the CC T2 in the AC alloys TT4, TT8 and TT6 was higher than one and lower than one when B was in synergy with Hf or Ta (silicide in the alloys TT7-AC and TT5-AC). The said ratio of the CC T2 was higher than one in the HT alloys TT5, TT6 and TT8 (i.e., when B was in synergy with Ta, Sn or Mo) and less than one in TT7-HT. The range of values of the Nb/Ti and Nb/(Ti + Hf) ratios was slightly higher compared with the second group of alloys, namely 1.9 to 0.67 compared with 2.12 to 0.76 (Figures 2b and 3b).

Compared with the silicide in the alloy TT4-AC, the synergy of B with Hf gave the highest VEC (4.324) in the CC T2 in the alloy TT7-AC, and the highest VEC (4.362) in the

"conventional" T2 in the alloy TT8-HT (synergy of B with Mo), see Figure 3c. The parameter VEC was less than 4.2 only when B was in synergy with Hf, Mo or Sn, respectively in CC T2 (in the alloy TT7-HT), CC Ti-rich T2 (alloy TT8-AC) and CC Ti-rich T2 (alloy TT6-HT). The range of the parameter VEC of T2 was 4.362 to 4.107, compared with the ranges 4.452 to 4.266 and 4.402 to 4.173, respectively for the Nb_5Si_3 in the first group and the second group of alloys, i.e., it was wider but with smaller high and low values than these groups (compare Figures 1c, 2c and 3c).

Compared with the silicide in the basis alloy, the parameter $\Delta\chi$ of the CC T2 silicide in the AC alloys TT7 (Hf addition), and TT5 (Ta addition) increased and decreased in the alloy TT6-AC (Sn addition) and the alloy TT8-AC (Mo addition) (Figure 3d). The range of the values of the parameter $\Delta\chi$ of T2 was 0.3512 to 0.1034, compared with the ranges 0.4153 to 0.2241, and 0.399 to 0.128, respectively for the Nb_5Si_3 in the first group and the second group of alloys, i.e., it was wider only than the first group of alloys and had smaller high and low values than these groups (compare Figures 1d, 2d and 3d).

The map of the parameters VEC and $\Delta\chi$ of the T2 silicide in the alloys with the alloy TT4 as their basis is shown in Figure 3e. Note (i) similar trends for the basis alloy TT4 and for the additions of Hf, Sn or Ta, (ii) the maxima for Hf (0.296, 4.303) and Sn (0.190, 4.311) and for the basis alloy TT4 (0.2546, 4.338), (iii) that only with the addition of Hf or Ta the parameter $\Delta\chi$ exceeds 0.3 and (iv) that only with the addition of Mo or Ta the parameter VEC exceeds 4.35.

The fourth group/set of Nb_5Si_3 is for advanced RM(Nb)ICs and RM(Nb)ICs/RCCAs with additions of RM, TMs, Ge, Sn or Ge + Sn (meaning simultaneous addition of Ge and Sn), with/without Al addition and with different Ti, Al, Cr, Si or Sn concentrations. The reader who is interested to know why Ge, Sn or Ge + Sn additions are important for metallic UHTMs could refer to [1,2,24,27,65–67]. Data for this group is shown in Figure 4. In Figure 4a, the data for the Nb_5Si_3 in the alloys JN4 and JG6 shows the effect of the presence of Al in an alloy where Hf, Mo and Ti are in synergy with Sn (the "conventional" silicide is converted to CC), whereas the simultaneous addition of Ge and Sn in the alloy OHS1 could reverse the effect of Al in the cast microstructure in the absence of Hf and Mo in the alloy (compare the silicide in the alloys JN4, JG6 and OHS1-AC). The data for Nb_5Si_3 in the alloys JN2 and JN3 shows that in the absence of Al in the alloy, its Cr concentration is important as lower Cr concentrations promote "conventional" Nb_5Si_3 and Ti-rich Nb_5Si_3.

The data for the Nb_5Si_3 in the alloys JZ4 and JZ5 shows the effect of Ti concentration in the alloy and that higher Ti concentration promotes the CC silicide, whereas the data for the Nb_5Si_3 in the alloys OHS1 and JZ5 shows that the synergy of Hf, Mo, Ti and W with Ge + Sn also promotes the CC silicide as seen in Figure 4a. In other words, in RM(Nb)ICs/RCCAs the type of Nb_5Si_3, meaning "conventional" or CC, can be controlled via the Ti concentration, the simultaneous addition of Ge and Sn and the synergy of these solutes with the simultaneous addition of Al, Cr, Hf, Mo, Ti and W, which are solute additions that contribute to achieving a balance of properties [2,27]. Is the choice of RMs important?

Comparison of the data for the alloys JZ3 and JZ4 shows that the substitution of Mo with Ta stabilised the "conventional" Nb_5Si_3 after heat treatment and converted the "conventional" Ti-rich Nb_5Si_3 in the cast alloy to CC, whereas a comparison of JZ4 with JZ3+ shows that the increase in the Sn concentration in the latter converted the "conventional" Ti-rich Nb_5Si_3 to CC in the alloy [JZ3+]-AC, as seen in Figure 4a. In other words, the choice of RMs is important. In RM(Nb)ICs/RCCAs with simultaneous addition of Al and Cr (each at 5 at.%, nominal), Ge, Hf and Sn with Ti and RMs, the type of Nb_5Si_3 ("conventional" or CC) can be controlled with (i) the concentrations of Sn and/or Ti, and (ii) and the choice of the RM that would be in synergy with W in the alloy.

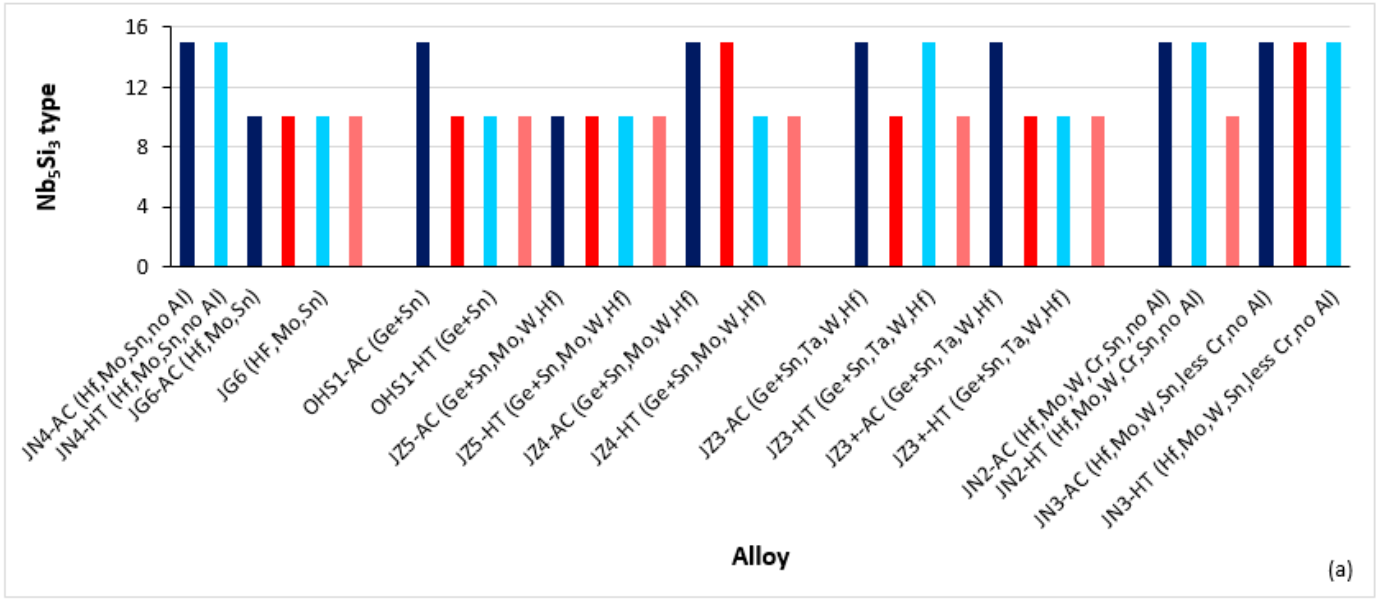
The synergies of solute additions had a strong effect on the Nb/Ti or Nb/(Ti + Hf) ratio of Nb_5Si_3, as seen in Figure 4b. For example, with the decrease in the Cr concentration in the alloy JN3, the Nb/(Ti + Hf) ratio of the "conventional" Nb_5Si_3 increased compared with the alloy JN2, whereas with the addition of Al in the alloy JG6, the Nb/(Ti + Hf) ratio not only decreased to less than two, compared with the alloy JN4 but also the ratio

was less than one for the CC Ti-rich Nb_5Si_3 in both the AC and HT conditions (hexagonal structure [68]). Similarly, the Nb/(Ti + Hf) ratio of CC Nb_5Si_3 decreased below two when the concentration of Ti in the alloy JZ5 increased compared with the alloy JZ4, in which the "conventional" Nb_5Si_3 had Nb/(Ti + Hf) higher than four. Furthermore, the substitution of Mo with Ta gave higher Nb/(Ti + Hf) ratios for the silicide in the alloy JZ3-HT compared with JZ4, but with the increase in the Sn concentration in the alloy [JZ3+]-HT, the said ratio was essentially the same as for the Nb_5Si_3 in the alloy JZ4-HT. In other words, the choice of solute additions and their concentrations is important not only for the type of Nb_5Si_3 but also for its Nb/(Ti + Hf) ratio.

Concentrations of solutes and synergies of the latter in advanced alloys affect the values of the parameters VEC and $\Delta\chi$ of Nb_5Si_3, Figure 4c,d. For example, with the addition of Al in the alloy JG6, the CC Ti-rich Nb_5Si_3 not only was hexagonal but also its parameter VEC decreased compared with the "normal" CC silicide in the same alloy and the "conventional" silicide in the alloy JN4, Figure 4c. However, the effect on VEC of the decrease in the Cr concentration in the alloy JN3 was minimal compared with the alloy JN2. The addition of Hf, Mo and W in JZ5 increased the parameter VEC of Nb_5Si_3 compared with the alloy OHS1, and the decrease in Ti concentration in JZ4 increased the parameter VEC further, as seen in Figure 4c. Changes of the parameter VEC of Nb_5Si_3 were marginal when the Mo was substituted with Ta in the alloy JZ3 compared with the alloy JZ4, but the increase in the Sn concentration in the alloy JZ3+ resulted to small decrease in the VEC of the CC silicide. The VEC range was from 4.584 for the "conventional" Nb_5Si_3 in the alloy JZ4-AC to 4.218 for the CC hexagonal Nb_5Si_3 in the alloy JG6-HT.

The parameter $\Delta\chi$ changed from 0.2055 for the CC Nb_5Si_3 in the alloy JG6-AC to 0.479 for the "conventional" Ti-rich Nb_5Si_3 in the alloy JN3, Figure 4d. The parameter $\Delta\chi$ was higher for the Al-free alloys JN2 and JN3, in which the Cr concentration had a noticeable effect on the parameter $\Delta\chi$ of the "conventional" Ti-rich Nb_5Si_3 in the alloy JN3. The simultaneous addition of Ge and Sn in the Hf free alloy OHS1 increased the parameter $\Delta\chi$ of Nb_5Si_3 compared with the alloys JN4 and JG6, and the addition of Mo and W increased further the parameter $\Delta\chi$. However, the increase in $\Delta\chi$ was marginal when the Ta was in synergy with W in the alloys JZ3 and JZ3+, even when the concentration of Sn was increased in the latter alloy.

The relationships between the parameters VEC and $\Delta\chi$ in Nb_5Si_3 in the alloys considered in Figure 4a are shown in the map in Figure 4e. Note (i) similar trends of the data for the alloys JN2 and JN4 (the lines are essentially parallel, with a shift to significantly lower $\Delta\chi$ in the W free and less rich in Cr alloy JN4), (ii) similar trends of the data for the alloys JG6, OHS1, JZ4 and JZ5, and JN3 with (a) a significant shift to higher VEC and $\Delta\chi$ values as the concentration of Cr was reduced and Al was removed from the alloy JN3 compared with the alloy JG6, (b) a gradual shift to higher VEC and $\Delta\chi$ values with Ge + Sn in the absence of Hf and Mo (alloys JG6 and OHS1), and when Hf, Mo and W were added to the alloys JZ4 and JZ5 with the simultaneous addition of Ge and Sn, (iii) opposite trend of the data when Mo was substituted with Ta in the alloys JZ3 and JZ3+, (iv) maxima in the data for JG6 (0.2506, 4.352), OHS1 (0.3061, 4.413), JZ4 and JZ5 (0.3343, 4.522), JN3 (0.4342, 4.556) and minimum (0.2841, 4.408) for the data of the alloys JZ3 and JZ3+. The relationship between the Nb/Ti or Nb/(Ti + Hf) ratio and the parameter VEC of Nb_5Si_3 is shown in Figure 4f. High ratio values link with high VEC values of the silicide, as was noted earlier in Figures 1f and 2f. Note the higher slope of the data for the Ta-containing alloys JZ3 and JZ3+ in Figure 4f, in the same way as the data for the alloy TT5 (Ta addition) in the Nb/Ti or Nb/(Ti + Hf) versus VEC map of alloys with TT4 as basis.



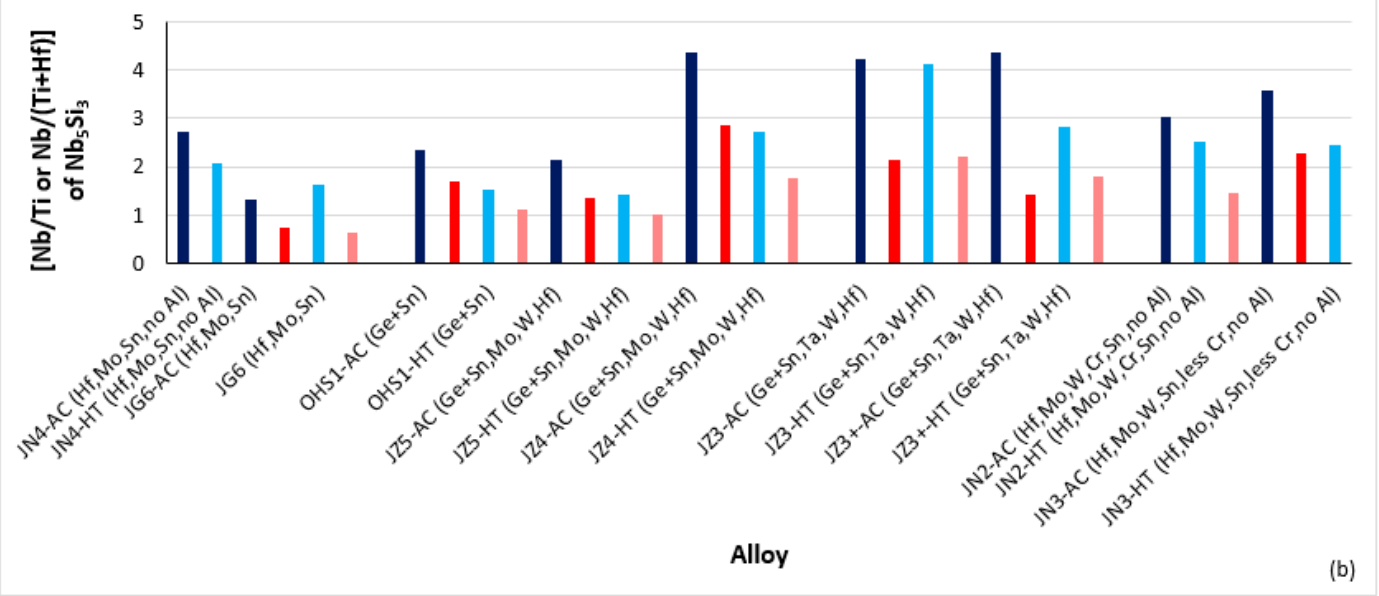
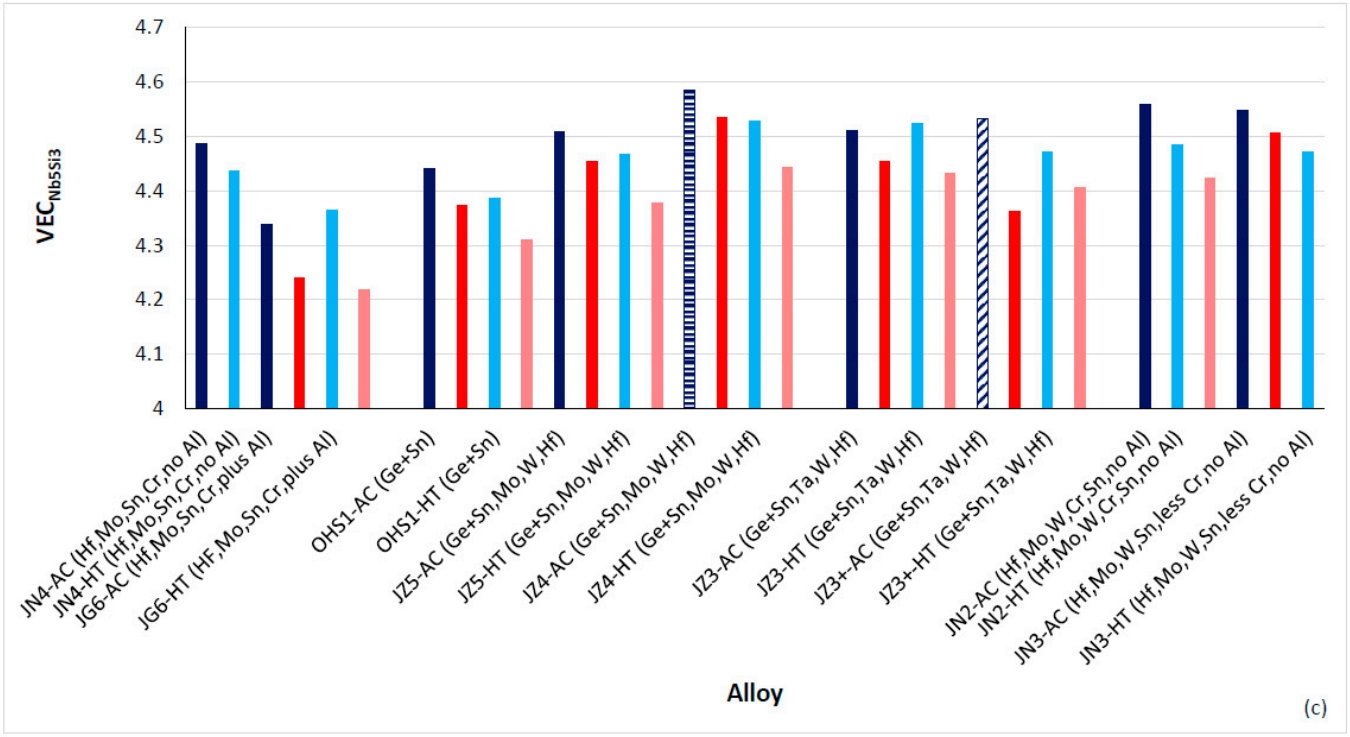


Figure 4. *Cont.*



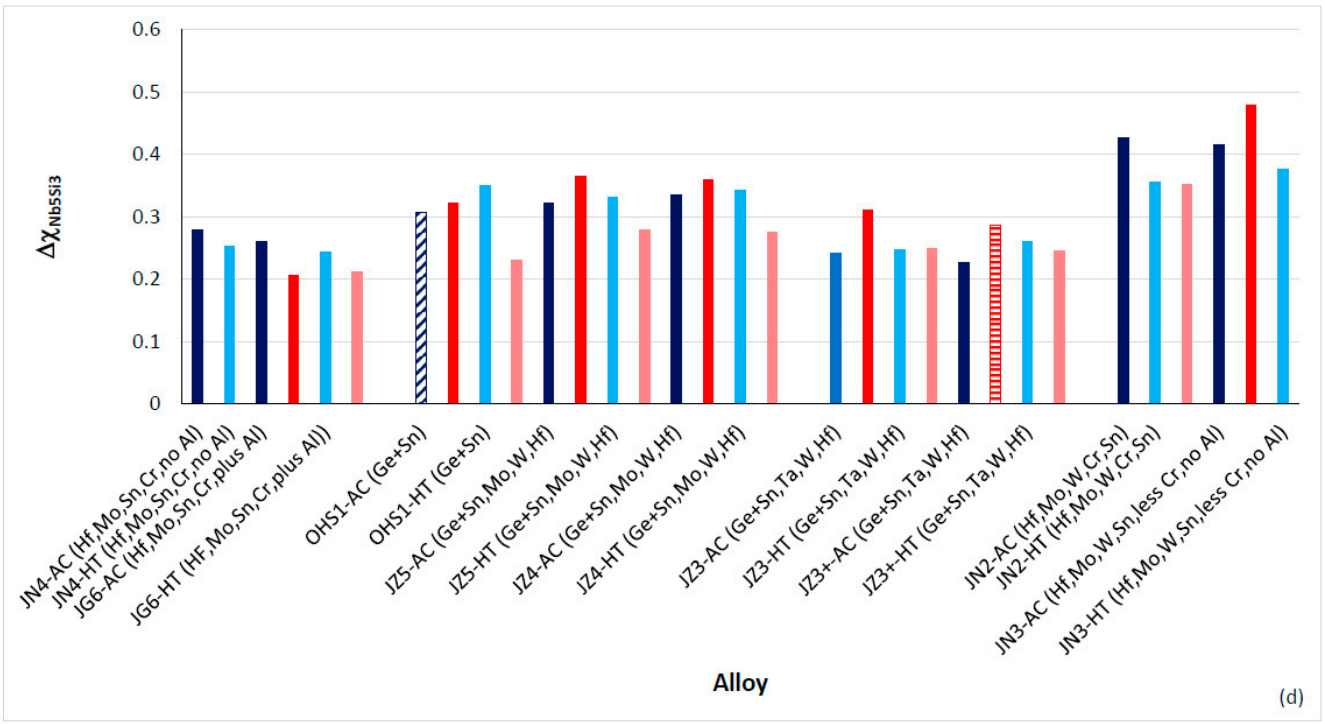
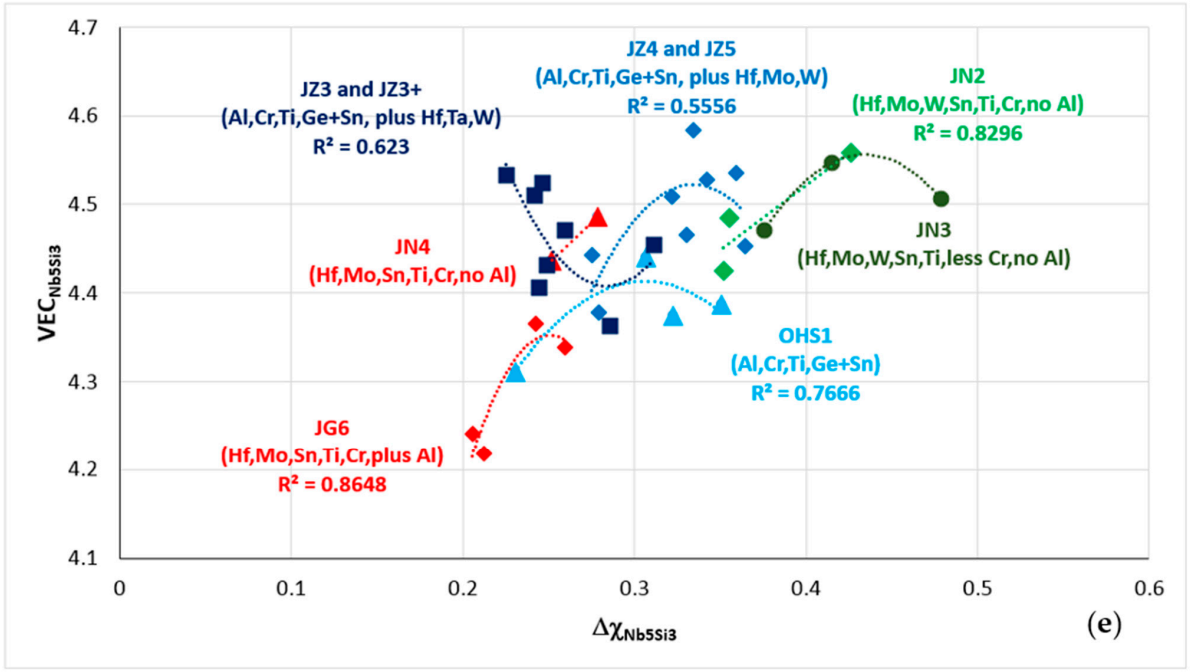


Figure 4. *Cont.*



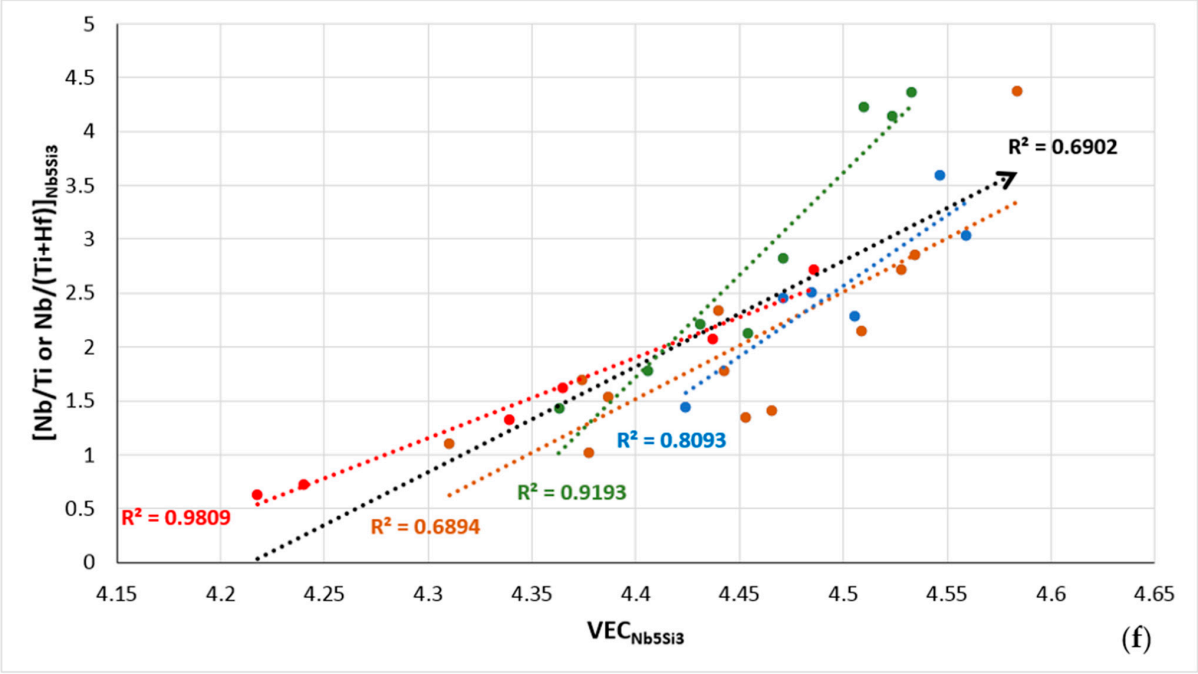


Figure 4. Data for Nb_5Si_3 in RM(Nb)ICs and RM(Nb)ICs/RCCAs with additions of RM, TMs, Ge, Sn or Ge + Sn, with/without Al addition and with different Ti, Al, Cr or Sn concentrations. Alloys JN2, JN3, JN4, JN4, JG6, JZ3, JZ3+, JZ4, JZ5 and OHS1. For nominal alloy compositions and references, see the Appendix B. (**a**) Type of Nb_5Si_3 ("conventional" or CC) and dark and lighter colours, respectively for the AC and HT conditions. For presentation purposes, the "values" 15 and 10 have been assigned, respectively to "conventional" Nb_5Si_3 and CC Nb_5Si_3. (**b**) Nb/Ti or Nb/(Ti + Hf) ratio of Nb_5Si_3, (**c**) VEC of Nb_5Si_3, (**d**) Δχ of Nb_5Si_3, (**e**) VEC versus Δχ of Nb_5Si_3 and (**f**) Nb/Ti or Nb/(Ti + Hf) ratio versus VEC of Nb_5Si_3. In (**e**), linear fit of data for the alloys JN2 and JN4, and the R^2 values are for parabolic fit of data. In (**f**), R^2 = 0.6902 for all data, R^2 = 0.9809 for the alloys JN4 and JG6, R^2 = 0.8093 for the alloys JN2 and JN3, R^2 = 0.9193 for the alloys JZ3 and JZ3+, R^2 = 0.6894 for the alloys OHS1, JZ5 and JZ4. In (**d**,**e**), the parameter Δχ is based on the Pauling electronegativity. See text for hatched data in (**c**,**d**) and for the arrow in (**f**). RM(Nb)ICs/RCCAs the alloys JG6, JZ3+, JZ4, JZ5 and OHS1.

2.1. Creep

In the microstructures of RM(Nb)ICs, RM(Nb)ICs/RCCAs or RM(Nb)ICs/RHEAs, the Nb_5Si_3 silicide is desirable because of its creep properties and its high Si content, which is expected to benefit oxidation resistance. As we discussed in the previous section, in the aforementioned metallic UHTMs, the Nb_5Si_3 is alloyed, and its alloying behaviour is described by its parameters VEC and $\Delta\chi$ [40]. TMs and RMs substitute Nb and simple metal and metalloid elements substitute Si [40]. Experiments have confirmed that the alloying of Nb_5Si_3 affects its creep properties [30–32,35,36,40].

Data for the creep of Nb_5Si_3 is limited. In the Norton plot of Nb_5Si_3 (Figure 12 in [40] and Figure 7 in [24]), the experimental data shows that the steady-state creep rate ($\acute{\varepsilon}$) of Nb_5Si_3 increases with alloying additions and that the alloying of Nb_5Si_3 causes the Norton line to shift upwards and to the left, i.e., towards higher creep rate at lower stress. In Figure 5, ln$\acute{\varepsilon}$ is plotted versus the parameter $\Delta\chi$ or VEC of the silicide and the data is for unalloyed Nb_5Si_3 and 3 alloyed silicides for which experimental data is available. The data is (i) for Nb_5Si_3 silicides where Nb is substituted either by Ti or by Ti and other TMs, and the Si is not substituted or is substituted with Al and B, i.e., the data is for $(Nb, TM)_5(Si, X)_3$, where TM = Cr, Hf, Ti and X = Al, B (see figure caption) and (ii) for a particular temperature and stress (T = 1200 °C and σ = 140 MPa). The arrow points in the direction of increasing creep rate for the specific T and σ. The data shows that the creep rate of $(Nb, TM)_5(Si, X)_3$ would increase as the alloying of Nb_5Si_3 changes the crystal structure of the silicide from tetragonal to hexagonal (the crystal structure of the T2 silicide is tetragonal and of the $D8_8$ silicide is hexagonal).

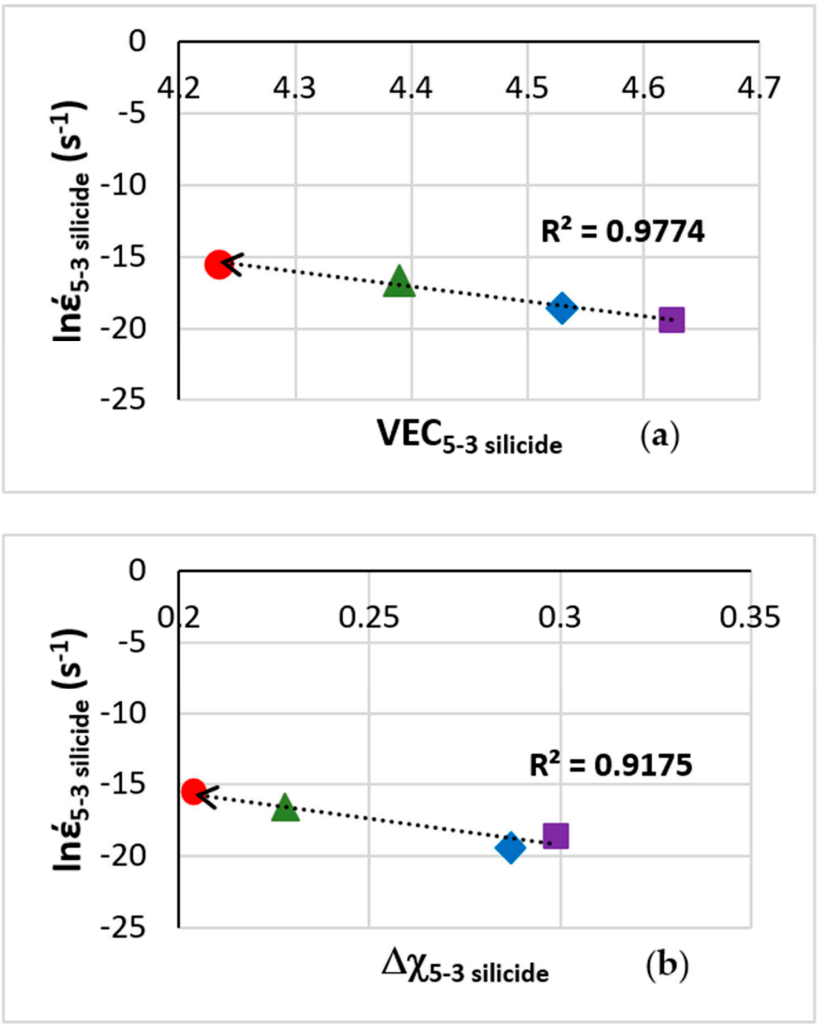


Figure 5. In $\acute{\varepsilon}$ versus the parameter, (**a**) VEC and (**b**) $\Delta\chi$ of unalloyed Nb_5Si_3 (squares), Ti alloyed $(Nb, Ti)_5Si_3$ (diamonds), B alloyed tetragonal T2 (triangles) and B alloyed hexagonal $D8_8$ (circles) 5–3 silicides.

Creep rate (compressive creep) for T = 1200 °C and σ = 140 MPa. Data from [24,40,74]. Ti-alloyed Nb_5Si_3 = 53 Nb-10 Ti-37 Si, B-alloyed T2 = 38.5 Nb-16 Ti-6 Hf-1 Cr-37 Si-1 Al-0.5 B, B-alloyed $D8_8$ = 41.5 Nb-13 Ti-3 Hf-4 Cr-12.5 Si-25.5 B-0.5 Al (at.%). In (**b**), the parameter Δχ is based on the Pauling electronegativity.

The arrow in Figure 5 points from the unalloyed past (purple square) towards the alloyed future of Nb_5Si_3 in metallic UHTMs, as in some sequences where Ti and Ti plus other TMs and RMs, such as Cr, Hf, Mo, Ta, V or W, substitute Nb, and Al, B, Ge or Sn substitute Si, owing to these additions in multiphase metallic UHTMs [1,2,24,40,73]. Note that previously the direction of change of the alloying behaviour of Nb_5Si_3 was represented with arrows in the Δχ versus VEC map in Figure 6 in [27]. The arrows showed in which direction the parameters of the silicide changed when different solutes substituted Nb or Si in the silicide.

In Figure 5, the arrow points in the direction of increasing creep rate for $(Nb, TM)_5(Si, X)_3$ at the given temperature and stress. There is no experimental data about the creep of Nb_5Si_3 where only Si is substituted by Ge or Sn, i.e., for $Nb_5(Si, Y)_3$, where Y = Ge, Sn. In this case, we know that the Δχ versus VEC map shows a different alloying behaviour of the latter silicides, meaning the change of alloying behaviour is in the opposite direction compared with the Ti-alloyed Nb_5Si_3 (see Figure 6 in [27] and Figure 11 in [40]). Currently, there is no experimental data for the creep of $Nb_5(Si, Y)_3$ silicides. In other words, we do not know whether the creep rate of these silicides also would increase with increasing temperature and stress. If creep experiments were to confirm this not to be the case, then I would like to suggest that further experimental work on the creep of tetragonal Nb_5Si_3 where Si is substituted with other simple metal and metalloid elements, namely with Al or with Al plus Ge or Sn, Ge + Sn or Al + Ge + Sn, and Nb with RMs (Mo, Ta, W) or Cr but not Hf or Ti, is essential.

The arrows in Figures 1f, 2f and 4f show that as the Nb/(Ti + Hf) ratio increases the parameter VEC increases. For RM(Nb)ICs, the said ratio has been shown to be important for their creep [24,35]. In alloys where the Nb/(Ti + Hf) ratio of the alloy and silicide is less than one, the creep rate is poor owing to hexagonal silicides being stable in the microstructure [68]. Low creep rates require the alloy Nb/(Ti + Hf) ratio to be higher than 1.4. Figure 1c,d, Figure 2c,d and Figure 4c,d show how the Nb/(Ti + Hf) ratio links (connects) with the parameters VEC and Δχ of the silicide. Below we shall see that the silicide can also link with the alloy and the solid solution via these parameters.

In Figures 1–4, the silicides with VEC and Δχ values closest to those of the unalloyed Nb_5Si_3 are shown with hatched data (the parameter VEC for the "conventional" silicide in the alloys KZ5-AC and ZX8-HT in Figure 1c, the parameter Δχ for the "conventional" silicide in the alloy ZX8-HT in Figure 1d, the parameter Δχ for the CC silicide in the alloy EZ8-AC and "conventional" silicide in the alloy EZ8-HT in Figure 2d, the parameter VEC for the "conventional" silicide in the alloy TT8-HT in Figure 3c, the parameter Δχ for the "conventional" silicide in the alloy TT8-AC in Figure 3d, the parameter VEC for the "conventional" silicide in the alloys JZ4-AC and [JZ3+]-AC in Figure 4c, the parameter Δχ for the "conventional" silicide in the alloy OHS1-AC and CC silicide in the alloy [JZ3+]-AC in Figure 4d). Note (i) that the solute additions in the aforementioned alloys are Al, B, Cr, Ge, Hf, Mo, Sn, Ta, Ti and W, all of which play a key role in the creep and oxidation of RM(Nb)ICs, RM(Nb)ICs/RCCAs or RM(Nb)ICs/RHEAs [1,2,24], (ii) that all the silicides in the alloys with basis the alloy JN1 have VEC lower than that of the unalloyed Nb_5Si_3 (Figure 2c) and (iii) the high Nb/(Ti + Hf) ratio of the hatched "conventional" silicides in the alloys [JZ3+]-AC and JZ4-AC (compare Figure 4a,b with c,d). With NICE, it is possible to design a material system consisting of a metallic UHTM substrate with the elements Al, Cr, Ge, Hf, Mo, Nb, Si, Sn, Ti and W and an environmental coating the bond coat of which would be alloy(s) of the Al-Cr-Hf-Nb-Si-Ti alloy system [2,15–17,67].

Why is the above important for the development of metallic UHTMs? Our research group has shown that NICE makes it possible to design a metallic UHTM to meet a specific property target, say creep or oxidation, with/without other constraints, for example, constraints about

solute elements, solute element ratios and hardness [2,15–17,24,27,50,51,62,64,66,67,75–79]. NICE also allows the alloy designer to consider alloying additions (meaning type and concentration) in the alloy to "move" its Nb_5Si_3 in a direction of change closer to or away from the creep properties of unalloyed Nb_5Si_3 or Ti-alloyed Nb_5Si_3, even to change the crystal structure of Nb_5Si_3. In other words, data about alloying behaviour and creep can be used to guide alloy design because the "bread and butter" of NICE are the relationships between solutes, between solute concentrations and alloy parameters, between alloy parameters and phase parameters and between alloy or phase parameters and their properties, where phase includes "conventional" and CC and/or HE phases (bcc solid solution, 5–3 silicides, C14-Laves phases, A15 compounds, eutectics of solid solutions and silicides) and alloy means RMIC, RCCA or RHEA with Nb and Si additions [1,2,15–17,24,27,40,44,49,51,58,61,62,66,67,80].

2.2. Hardness

According to the alloy design methodology NICE, the hardness of Nb_5Si_3 can be expressed as a function of its parameter VEC with the linear relationship $HV_{Nb5Si3} = a_1VEC_{Nb5Si3} + b_1$ (e.g., see Figure 14 in [27]). Guided by NICE, relationships of the parameter VEC with key solutes in the Nb_5Si_3 were sought in order to find out if the hardness of the silicide can be written down as a function of solute additions in metallic UHTMs. It was discovered that the parameter VEC of Nb_5Si_3 is related to its Nb/(Ti + Hf) ratio with a linear relationship $[Nb/(Ti + Hf)]_{Nb5Si3} = a_2VEC_{Nb5Si3} + b_2$, where the constants a_2 and b_2 depend on the basis alloy (see Figures 1f, 2f and 4f). For the basis alloy KZ5, the constants are $a_2 > 0$ and $b_2 < 0$. For KZ series alloys (for example, see the alloys in [58,64,76,80–83]), $a_1 < 0$ and $b_1 > 0$ (Figure 14a in [27]), i.e., the hardness of the silicide decreases as its parameter VEC increases. (Note that the hardness of carbides, nitrides and carbo-nitrides of TMs decreases with their parameter VEC [84] and that the hardness of Ti-alloyed Nb_5Si_3, i.e., of $(Nb, Ti)_5Si_3$, decreases and increases with its parameter VEC, respectively for $\alpha(Nb, Ti)_5Si_3$ and $\beta(Nb, Ti)_5Si_3$ (see Figures 15 and 16 in [49])).

The hardness of Nb_5Si_3 can be written as a linear function of the ratio $X_{Nb5Si3} = Nb/(Ti + Hf)$, i.e., $HV_{Nb5Si3} = (a_1[X_{Nb5Si3} - b_2]/a_2) + b_1$ or $HV_{Nb5Si3} = f_1(X_{Nb5Si3})$. Given that in NICE the concentrations of the solute elements in Nb_5Si_3 are related to the concentration of Hf or Ti in the silicide with linear relationships, e.g., $Si = c_1Ti + d_1$, $Hf = c_2Ti + d_2$ or $Hf = c_3Nb + d_3$, where the constants c_i and d_i can be positive or negative (e.g., see [24,40,76]), the ratio X_{Nb5Si3} can be written as a function of the concentration of a specific solute and, therefore, the hardness of Nb_5Si_3 can also be written as a function of the concentration of a specific solute element in the silicide. In other words, the dependence of the hardness of Nb_5Si_3 on its parameter VEC allows one to calculate the HV_{Nb5Si3} (attributed to VEC) for the specific concentration(s) of a specific solute.

Furthermore, as a consequence of the relationships between the parameters VEC and $\Delta\chi$ of the silicide (Figures 1e, 2e, 3e and 4e), and thus between $X_{Nb5Si3} = Nb/(Ti + Hf)$ and $\Delta\chi_{Nb5Si3}$, and, therefore, $X_{Nb5Si3} = a_3\Delta\chi_{Nb5Si3} + b_3$, where a_3 and b_3 can be positive or negative (e.g., for KZ5 as the basis alloy see Figure 1g). NICE hinted that electronegativity is also important for the hardness of the silicide. Indeed, $HV_{Nb5Si3} = (a_1[X_{Nb5Si3} - b_2]/a_2) + b_1$ or $HV_{Nb5Si3} = f(\Delta\chi_{Nb5Si3}) = (a_1[a_3\Delta\chi_{Nb5Si3} + b_3 - b_2]/a_2) + b_1$. The hardness of Nb_5Si_3 can increase or decrease with increasing parameter $\Delta\chi$ depending on the solute elements. Given that the Ti content of Nb_5Si_3 depends on its parameter $\Delta\chi_{Nb5Si3}$ (i.e., $\Delta\chi_{Nb5Si3} = g(Ti_{Nb5Si3})$) with linear relationships, $\Delta\chi_{Nb5Si3} = a_4Ti + b_4$ where a_4 and b_4 can be positive or negative, and the hardness $HV_{Nb5Si3} = (a_1[a_3(a_4Ti + b_4) + b_3 - b_2]/a_2) + b_1$ (in other words, the HV_{Nb5Si3} is a function of its Ti content). Owing to the relationships of the concentrations C_i^{Nb5Si3} of solutes i in Nb_5Si_3 with its Ti content (i.e., $C_i^{Nb5Si3} = g_i(Ti_{Nb5Si3})$) (e.g., $Si = c_1Ti + d_{1,\,etc.}$, see above), the hardness of alloyed Nb_5Si_3 for different solutes can be calculated. Actually, the dependence of the hardness of Nb_5Si_3 on its parameter $\Delta\chi$ allows one to calculate the HV_{Nb5Si3} (attributed to $\Delta\chi$) for the specific concentration(s) of a specific solute.

The experimental Vickers hardness of unalloyed βNb_5Si_3 is 1360 HV [40]. First principles calculations have shown that the substitution of Nb by Ti in the $\beta(Nb, Ti)_5Si_3$ reduces

the hardness [40,85]. The experimental Vickers hardness of the β(Nb, Ti, Cr)$_5$(Si, Al)$_3$ in KZ5-AC was 1131 HV [76] of the β(Nb, Ti, Cr, Hf)$_5$(Si, Al)$_3$ in JN1-HT was 1124 HV [76] and of the β(Nb, Ti, Cr)$_5$(Si, Al, Ge)$_3$ in ZF6-HT was 1576 HV [64]. To put it in another way, the alloying of the silicide and the synergies of solutes in the alloys KZ5, JN1 and ZF6, respectively reduced and increased the hardness of the alloyed βNb_5Si_3 in these alloys. The concentrations of solutes in Nb_5Si_3 in the aforementioned alloys are known (determined using EPMA, see [64,76,81]), thus it is possible to calculate the hardness of the silicide (attributed to VEC or Δχ) for the concentration (at.%) range of each solute, see Tables 1 and 2. The calculated hardness of alloyed βNb_5Si_3 is given in Table 1 and the concentration ranges of each solute in the silicide that were determined using EPMA are given in Table 2.

Table 1. Calculated with NICE contributions of solutes to the Vickers hardness of alloyed βNb_5Si_3 attributed to the parameters Δχ and VEC for the silicide in the alloys KZ5-AC, JN1-HT and ZF6-HT (for the concentration ranges of each solute see the EPMA data in Table 2).

Alloy and Parameter		Solute						
		Al	Cr	Ge	Hf	Nb	Si	Ti
KZ5-AC	Δχ	1234–1279	1220–1350	-	-	1013–1326	1176–1225	1024–1469
	VEC	1385–1411	1403–1471	-	-	793–1398	1270–1311	1185–1495
JN1-HT	Δχ	1216–1341	1265–1321	-	955–1528	922–1576	1303–1365	887–1563
	VEC	1331–1390	1359–1409	-	1155–1263	1213–1578	1263–1301	1253–1525
ZF6-HT	Δχ	1174–1315	1252–1403	1328–1707	-	845–1158	1204–1297	1135–1658
	VEC	1385–1434	1418–1475	1448–1558	-	1102–1421	1397–1436	1365–1566

Table 2. Measured with EPMA (range and average) and calculated with NICE concentrations (at.%) of solutes in the alloyed βNb_5Si_3 in the alloys KZ5-AC, JN1-HT and ZF6-HT. EPMA data from [64,76,81].

Alloy	Method	Solute						
		Al	Cr	Ge	Hf	Nb	Si	Ti
KZ5-AC	EPMA	3.1–4	1.2–2.7	-	-	36.7–46.8	30.8–33.2	16.7–25.2
		3.5	2	-	-	41.9	31.8	23.9
	NICE	3.6	0.7	-	-	40.7	30.8	24.2
JN1-HT	EPMA	1.6–3.3	0.4–1.3	-	4.5–9.5	27.1–41.5	31.4–33.6	17.9–26.7
		3.1	1.2	-	9.3	27.3	32.5	26.6
	NICE	3.5	0.5	-	8.1	31.8	32.8	23.3
ZF6-HT	EPMA	3.1–5.2	1.5–2.8	7–8.1	-	35.9–43.4	20.8–24.4	20.5–29.7
		4.8	2.7	7.8	-	37.6	21	26.1
	NICE	3.9	1.1	7.7	-	35.4	25.2	26.8

For example, in the case of the β(Nb, Ti, Cr)$_5$(Si, Al)$_3$ in KZ5-AC, we have 16.7 < Ti < 25.2 at.%, 30.8 < Si < 33.2 at.%, 3.1 < Al < 4 at.%, 1.2 < Cr < 2.7 at.% and 36.7 < Nb < 46.8 at.% [81], and for each element, the calculated Vickers hardness (i) attributed to the parameter VEC is in the range 1185 to 1495, 1270 to 1311, 1385 to 1411, 1403 to 1471 and 793 to 1398 HV, respectively for Ti, Si, Al, Cr and Nb, and (ii) attributed to the parameter Δχ is 1024 to 1469, 1176 to 1225, 1234 to 1279, 1220 to 1350 and 1013 to 1326, respectively for Ti,

Si, Al, Cr and Nb. Compared with the unalloyed βNb_5Si_3, on account of VEC and $\Delta\chi$, the decrease in the hardness can be attributed, respectively to the solutes Nb, Si and Ti, and to all solutes among which Al, Cr and Si have a strong effect. Note that the average hardness calculated using the low hardness contribution of each element that is attributed to $\Delta\chi$ and VEC is 1133.4 and 1207.2, respectively (average 1170.3), compared with the measured hardness 1131 $\pm$ 54.

In the case of the alloy JN1-HT, the data in Table 1 shows that, compared with the unalloyed βNb_5Si_3 and taking into consideration the parameters VEC and $\Delta\chi$, the decrease in the hardness can be attributed, respectively to the solutes Nb, Si, Ti and Hf, and to all solutes among which Ti and Nb have a strong effect. However, the hardening attributed by the parameter $\Delta\chi$ to Hf can be significant at lower Hf concentrations. Note that the average hardness calculated using the low hardness contribution of each element that is attributed to the parameters $\Delta\chi$ and VEC is 1091.3 and 1262.3, respectively (average 1176.8), compared with the measured hardness 1124 $\pm$ 58. Regarding the alloy ZF6-HT, the data in Table 1 shows that, compared with the unalloyed βNb_5Si_3 and taking into account VEC and $\Delta\chi$, the increase in the hardness can be attributed, respectively to all solutes, in particular, Ge, and to Cr, Ge and Ti, with Ge having a noticeable hardening effect at high concentration, attributed to electronegativity ($\Delta\chi$). Note that the average hardness calculated using the high hardness contribution of each element that is attributed to the parameters $\Delta\chi$ and VEC is 1423 and 1481.7, respectively (average 1452.4), compared with the measured hardness 1576 $\pm$ 60.

In [40], it was discussed that different alloying additions affect in a different way the solubility ranges in Nb_5Si_3. Compared with the silicide in the basis alloy KZ5, the data in Table 2 shows that with the addition of Hf in the alloy JN1, the Ti and Si concentration ranges increased while those of Al, Cr and Nb decreased, whereas with the addition of Ge in the alloy ZF6, the Ti, Al and Cr concentrations ranges increased and those of Si and Nb decreased. These changes also contributed to the changes in the Vickers hardness of the alloyed βNb_5Si_3 in the alloys JN1 and ZF6, along with the alloying with Hf or Ge.

The relationships of the hardness of Nb_5Si_3 with its parameter $\Delta\chi$ ($HV_{Nb5Si3} = f(\Delta\chi_{Nb5Si3})$) and of $\Delta\chi_{Nb5Si3}$ with the Ti concentration in Nb_5Si_3 ($\Delta\chi_{Nb5Si3} = g(Ti_{Nb5Si3})$) in different RM(Nb)ICs, RM(Nb)ICs or RM(Nb)ICs/RHEAs, and the correlations of the concentrations C_i of solutes i with the Ti concentration in Nb_5Si_3 ($C_i^{Nb5Si3} = g_i(Ti_{Nb5Si3})$) allow us to calculate the chemical composition of the silicide using the measured hardness in the relationship between $HV_{Nb5Si3} = f_1(X_{Nb5Si3})$ and the $HV_{Nb5Si3} = f(\Delta\chi_{Nb5Si3})$ and $\Delta\chi_{Nb5Si3} = g(Ti_{Nb5Si3})$ and $C_i^{Nb5Si3} = g_i(Ti_{Nb5Si3})$ relationships in NICE. For the alloyed βNb_5Si_3 in the alloys KZ5-AC, JN1-HT and ZF6-HT, the measured chemical composition range and average concentration, and the calculated composition of each solute are given in Table 2. For each alloy, the agreement between measured and calculated concentrations of solutes in the silicide is good with the exception of the concentration of Cr that was underestimated by NICE for each alloy and the overestimated concentrations of Si and Nb in the alloys ZF6-HT and JN1-HT, respectively.

Given that $X_{Nb5Si3} = [Nb/(Ti + Hf)]_{Nb5Si3} = a_2VEC_{Nb5Si3} + b_2 = a_3\Delta\chi_{Nb5Si3} + b_3$, the relationship between the parameters VEC and $\Delta\chi$ of the silicide is $\Delta\chi_{Nb5Si3} = (a_2VEC_{Nb5Si3} + b_2 - b_3)/a_3$. For the basis alloy KZ5, the data gives $4.213 < VEC_{Nb5Si3} < 5.902$ for $\Delta\chi_{Nb5Si3} > 0$. Figure 1g is shows the extension of the brown data linear fit. The intercepts of the linear fits of the blue and black data, black and brown data and blue and brown data, respectively are (0.353, 2.859), (0.354, 2.891) and (0.355, 2.874), and the intercept of the linear fit of the dark green colour data (i.e., the data for CC Nb_5Si_3, see Figure 1g caption) of the green parabola is (0.354, 1.959). Note that data converge to similar $\Delta\chi$ (about 0.354) and that the ratio values (about 2.9 and 2) correspond to high VEC in Figure 1f. From $\Delta\chi_{Nb5Si3} = 0.354$ and the linear fits of data in Figure 1g (i.e., the blue, black and brown lines), we get the ratio $[Nb/(Ti + Hf)]_{Nb5Si3}$ and using Figure 1f, we calculate the parameter $VEC_{Nb5Si3} = 4.513$. When we use the linear fits of the dark green colour data (i.e., the data for CC Nb_5Si_3, see Figure 1g caption) of the green parabola, we get the VEC_{Nb5Si3} values 4.382 and 4.422, respectively for the linear fit with positive and negative slope. Parabolic fits of the blue and brown data, and of the black and brown data gave $R^2 = 0.9056$

and R^2 = 0.8863, respectively. The maxima for these parabolas and for the green data, respectively are (0.3163, 2.651), (0.3592, 2.5248) and (0.3628, 1.7128), and give VEC_{Nb5Si3} values 4.49, 4.48 and 4.4, respectively. Note that the VEC_{Nb5Si3} for the silicides in KZ5-AC and ZX8-HT shown with hatched data in Figure 1c was 4.45.

2.3. Alloy Design

As discussed in [2,51,56] and in this paper, in RM(Nb)ICs, RM(Nb)ICs/RCCAs or RM(Nb)ICs/RHEAs "conventional" phases can co-exist with CC or HE phases. NICE can design the aforementioned metallic UHTMs with said phases owing to relationships between parameters of alloys and phases [24]. Such relationships are characteristic of the approach to alloy design put into practise with NICE. Figure 6 shows examples of such relationships between the parameter VEC of alloy and "conventional" silicide (Figure 6a), between the parameters $\Delta\chi$ and VEC of CC silicide (Figure 6b), and between the parameter VEC of CC Nb_{ss} and Nb_5Si_3 (Figure 6c).

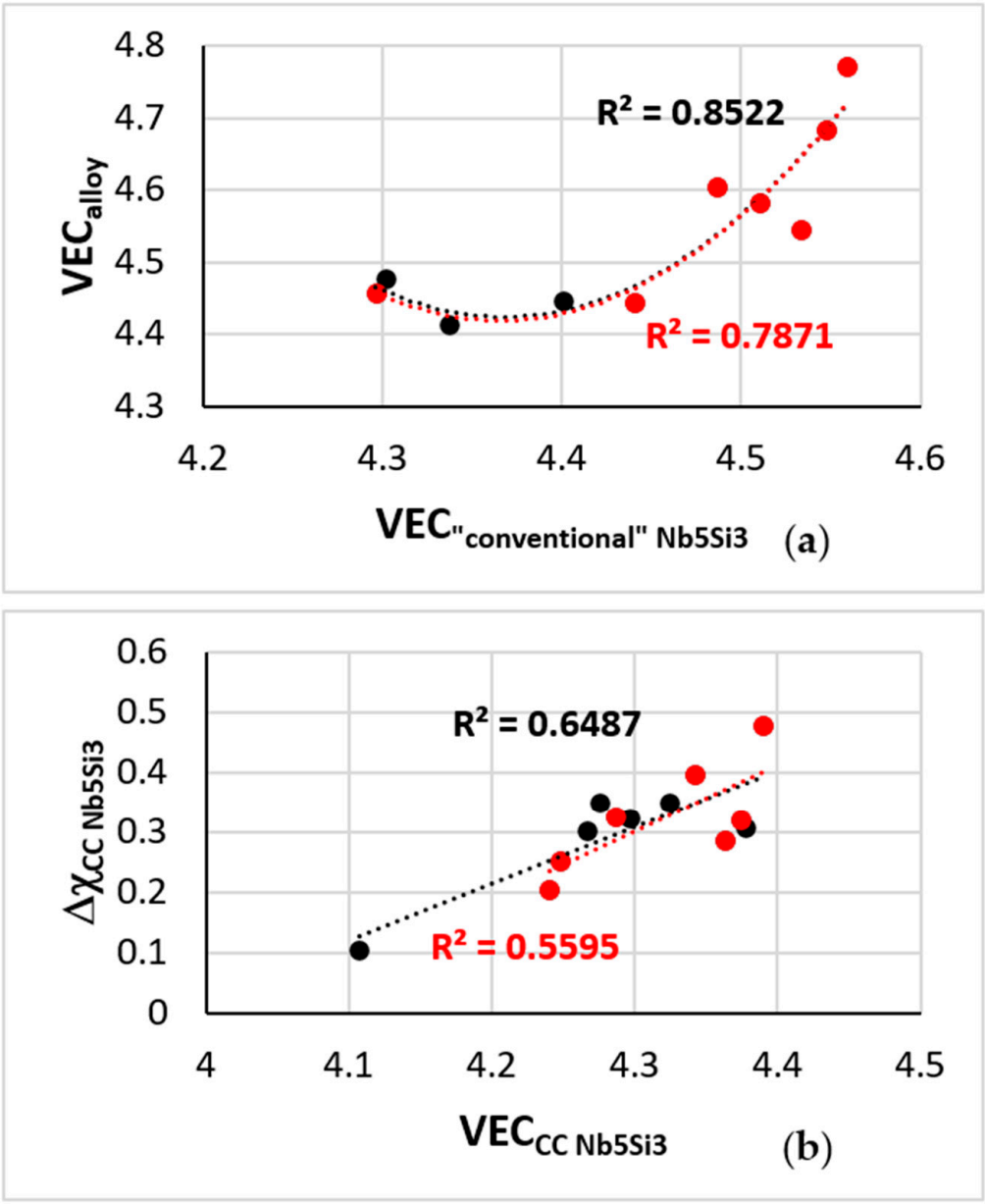


Figure 6. *Cont.*

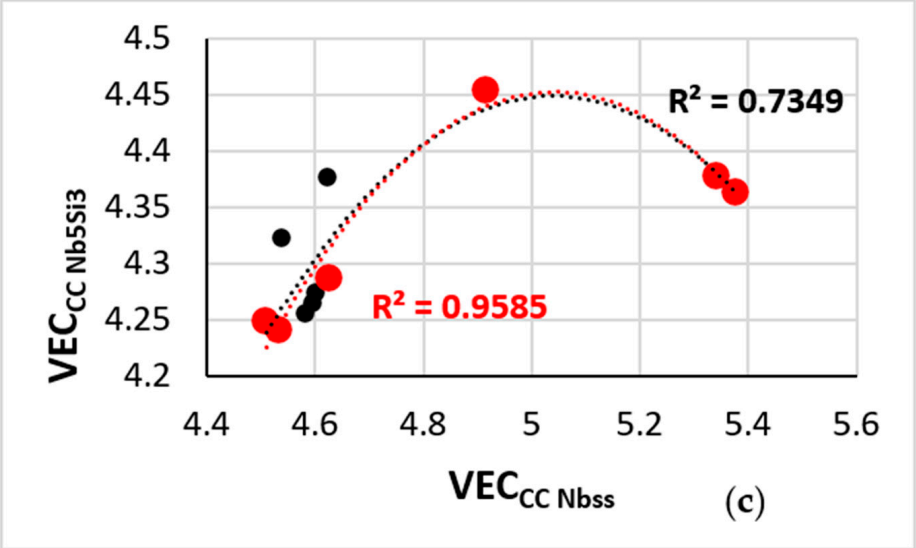


Figure 6. Relationships between the parameters (**a**) VEC of alloy versus VEC of "conventional" Nb_5Si_3, (**b**) $\Delta\chi$ versus VEC of CC Nb_5Si_3 and (**c**) VEC of CC Nb_5Si_3 versus VEC of CC Nb_{ss}. In (**a**), AC alloys JN1, JN2, JN3, JN4, JZ3, JZ3+, OHS1, TT4, TT8 and ZF6, in (**b**) AC alloys EZ8, JN1, JG6, JZ3, JZ3+, KZ6, OHS1, TT4, TT5, TT7, TT8, ZF6 and ZF9 and in (**c**), AC alloys EZ8, JG6, JZ3, JZ3+, KZ6, TT4, TT5, TT7 and ZF9, and HT alloys JZ5 and TT5. In all three parts, the red data is for alloys with Ge and/or Sn addition. Black R^2 values are for all data. Parabolic fits of data in (**a**,**c**). For nominal alloy compositions and references, see the Appendix B.

Regarding phases other than the Nb_5Si_3 silicide and their properties, for example, the bcc solid solution(s) or eutectics consisting of bcc solid solution and Nb_5Si_3, and properties of RM(Nb)ICs, RM(Nb)ICs/RCCAs and RM(Nb)ICs/RHEAs, for example, oxidation, creep, hardness or specific strength, other "arrows of alloying" also link with other properties.

For example, the hardness of the solid solution (HV_{ss}) increased and decreased as its parameter δ_{ss} increased, respectively for B-free and B-containing RM(Nb)ICs and RM(Nb)ICs/RCCAs, see Figure 4 in [2]. We could choose the "arrow of hardness" of the bcc solid solution to point, respectively, in the direction of increase and decrease in HV_{ss} with δ_{ss} for the alloys in Figure 4 in [2]. In the case of B-free alloys, the δ_{ss} increased with increasing $(Ge + Sn)_{ss}$ (Figure 7b in [56]). Note that Ge and Sn are two solutes that play a key role in the oxidation of metallic UHTMs with Nb and Si addition [1,2,65–67]. We could choose the "arrow of alloying" to point in the direction of increase in δ_{ss} in Figure 7b in [56]. However, because the $(Ge + Sn)_{ss}$ sum links with the concentrations of other solute additions (see Figure 9 in [56]), the "arrow of alloying" also "targets" other solute additions. Furthermore, because δ_{ss} increased with increasing $[O]_{ss}$ (see Figure 11 in [56]), the effect of the contamination of the bcc solid solution on its hardness also can be taken into account via the "arrow of alloying". In the case of B-containing alloys, the δ_{ss} increased with increasing boron in the solid solution, B_{ss} (Figure 7a in [56]). Note that B is another solute that plays a key role in the oxidation of metallic UHTMs with Nb and Si addition [1,2,61,62]. We could choose the "arrow of alloying" to point in the direction of increase in δ_{ss} in Figure 7a in [56]. Similarly, with the $(Ge + Sn)_{ss}$ sum, the B_{ss} is linked with the concentrations of other solute additions (Figure 8 in [56]), and thus the "arrow of alloying" also "targets" other solute additions. Note the opposite trends regarding relationships of solute concentrations with $(Ge + Sn)_{ss}$ or B_{ss} (compare Figures 8 and 9 in [56]).

The hardness of RM(Nb)ICs and RM(Nb)ICs/RCCAs with B, Ge or Sn addition (HV_{alloy}) increased with the parameter VEC_{alloy} (Figure 11 in [27]). Additionally, the room temperature-specific strength of RM(Nb)ICs and RM(Nb)ICs/RCCAs decreased with increasing VEC_{alloy} (Figure 6 in [2]). Furthermore, there are relationships between the steady-state creep rate of RM(Nb)ICs at a specific temperature and stress and the parameters

VEC_{alloy}, $\Delta\chi_{alloy}$ or δ_{alloy} (Figure 10 in [24]). We could choose the "arrow of alloy hardness" to point in the direction of increase in VEC_{alloy} for alloys with B, Ge or Sn addition, the "arrow of alloy specific strength" to point in the direction of decrease in VEC_{alloy} and the arrow that shows the change of alloy creep to point in the direction of increasing VEC_{alloy} or $\Delta\chi_{alloy}$ and decreasing δ_{alloy}. "Arrows of oxidation" were shown in the VEC_{alloy} versus $(\Delta W/A)_{alloy}$ in Figure 16 in [27] ($(\Delta W/A)_{alloy}$ is the mass change in isothermal oxidation in air at 1200 °C of RM(Nb)ICs and RM(Nb)ICs/RCCAs). The parameter VEC_{alloy} links with solute concentrations in the alloy and bcc solid solution, for example, see the VEC_{alloy} versus Al_{ss} and Al_{alloy} versus Al_{ss} relationships in Figure 19 in [27] and the VEC_{alloy} versus Al_{alloy} and VEC_{ss} versus Al_{ss} relationships in Figure 18 in [27], and relationships between solute concentrations and alloy steady-state creep rate for the creep goal conditions, as seen in Figure 22 in [27]. In each of the aforementioned figures, we could assign an "arrow of alloying". Furthermore, we could give "arrows of alloying" for the relationships between VEC_{alloy} and VEC_{ss} or VEC_{Nb5Si3} in Figure 17 in [27].

The hardness of eutectics with bcc solid solution and Nb_5Si_3 ($HV_{eutectic}$) increased with increasing parameter $VEC_{eutectic}$ (Figures 12 and 13 in [49]) and decreased with increasing parameter $\Delta\chi_{eutectic}$ or $\delta_{eutectic}$ (Figure 15 in [27]). We could choose the "arrow of eutectic hardness" to point in the direction of increase in $VEC_{eutectic}$ or decrease in $\Delta\chi_{eutectic}$ or $\delta_{eutectic}$. "Arrows of alloying" can be assigned to the relationships between $VEC_{eutectic}$ and $<Si>_{eutectic}$ (Figure 14 in [49]), between $\delta_{eutectic}$ and $<Si>_{eutectic}$ (Figure 8 in [49]), between $\Delta\chi_{eutectic}$ and $<Si>_{eutectic}$ (Figure 6 in [49]), where $<Si>_{eutectic}$ = Al + Ge + Si + Sn, between $\Delta\chi_{eutectic}$ and $VEC_{eutectic}$ (Figure 5 in [49]) and $\Delta\chi_{eutectic}$ and $\Delta\chi_{alloy}$ (Figure 17 in [27]).

The "arrows of alloying" and arrows of properties, for example, in Nb_5Si_3 steady-state creep rate, solid solution hardness, eutectic hardness, alloy hardness, alloy specific strength, alloy steady-state creep rate and alloy oxidation, by having specific properties such as their "targets", point the alloy developer to the direction of appropriate and trustworthy paths and guide him/her along these paths in an alloy development roadmap/"landscape". The starting point in NICE is always a property goal or property goals if a balance of properties were to be the desirable outcome of alloy design/development [24].

NICE informs (warns) the alloy developer (a) that it is unrealistic to seek to develop an alloy that meets simultaneously the three specific property goals for toughness, creep and oxidation [1,2], (b) that there is no point in arbitrarily choosing some elements from the periodic table and putting them to "work together" (be in synergy) at some arbitrarily chosen concentrations [27] because synergies differ (e.g., see Figure 4e,f) and chemical composition and element identity matter because they "bring into being" parameter values [1,2,24,27,40,44,49,55,73] and (c) that the development of metallic UHTMs should work closely together with the development of environmental coatings [1,2,15–17,27,78,79].

3. Conclusions

Different types of alloyed "normal" Nb_5Si_3 and Ti-rich Nb_5Si_3, namely "conventional", CC or HE, can form in metallic UHTMs with Nb and Si addition, i.e., in RM(Nb)ICs, RM(Nb)ICs/RCCAs and RM(Nb)ICs/RHEAS. Alloying behaviour and properties of the silicides can be studied using their Nb/(Ti + Hf) ratios, the parameters VEC and $\Delta\chi$ and relationships between them.

1. Ti-rich $(Nb, Ti, Cr)_5(Si, Al)_3$, is converted from "conventional" to CC when it is alloyed with B, Ge, Hf, Mo, Sn or Ta. With the exception of the B addition, the "conventional" Nb_5Si_3 has VEC > 4.4. The "conventional" and CC Nb_5Si_3 has the lowest and highest $\Delta\chi$ when it is alloyed with B or Ge.
2. Ti rich $(Nb, Ti, Cr, Hf)_5(Si, Al)_3$ is CC when alloyed with B, Ge, Mo or Sn and with the addition of B or Ge the "normal" and Ti rich silicide changes to CC in both the AC and HT conditions. The alloying of $(Nb, Ti, Cr, Hf)_5(Si, Al)_3$ with B, Ge, Mo or Sn gives Nb/(Ti + Hf) < 1.9.

3. Regarding the alloyed tetragonal T2-(Nb, Ti, Cr)$_5$(Si, Al, B)$_3$, the "conventional" T2 is stable in the HT condition when alloyed with Mo or Sn. When alloyed with Hf or Ta the T2 has $\Delta\chi > 0.3$ and when alloyed with Mo or Ta, it has VEC > 4.35.
4. In advanced metallic-UHTMs where Hf, Mo and Ti are in synergy with Sn, (i) the addition of Al converts the "conventional" silicide to CC, whereas (ii) lower Cr concentration promotes "conventional" Nb_5Si_3 and Ti-rich Nb_5Si_3 in the absence of Al in the alloy. Furthermore, in advanced metallic-UHTMs where Al, Cr, Hf, RMs and Ti are in synergy with Ge + Sn the type of Nb_5Si_3 depends (iii) on the concentrations of Sn and/or Ti, and (iv) the choice of RM that is in synergy with W in the alloy, in particular the substitution of Mo with Ta stabilizes the "conventional" Nb_5Si_3 after HT and converts the "conventional" Ti rich Nb_5Si_3 to CC.
5. The steady-state creep rate of the alloyed silicide can be related to its parameters VEC and $\Delta\chi$, and its Nb/(Ti + Hf) ratio. For a given temperature and stress, the steady-state creep rate of the alloyed silicide, in which TMs substitute Nb and Al and B substitute Si, increases with decreasing parameter and ratio value, compared with the unalloyed Nb_5Si_3.
6. Relationships of the hardness of alloyed Nb_5Si_3 with its parameter VEC, relationships of the latter with the silicide parameter $\Delta\chi$ and Nb/(Ti + Hf) ratio and relationships of the concentrations of solutes in the silicide with its Ti concentration enable the alloy designer/developer (i) to calculate the hardness of alloyed Nb_5Si_3, attributed to VEC or $\Delta\chi$ for a specific solute and its concentration range and (ii) to calculate the average chemical composition of Nb_5Si_3 from its hardness.

Funding: This research received funding from the EPSRC (EP/H500405/1, EP/L026678/1).

Data Availability Statement: All the data for this work is given in the paper and cited references, other data cannot be made available to the public.

Acknowledgments: The support of this work by the University of Sheffield, Rolls-Royce Plc and EPSRC (EP/H500405/1, EP/L026678/1) is gratefully acknowledged. For the purpose of open access, the author has applied a 'Creative Commons Attribution (CC BY) licence to any Author Accepted Manuscript version arising.

Conflicts of Interest: The author declares no conflict of interest.

Appendix A. Abbreviations Used in the Paper

AC	as cast
CC	complex concentrated or compositionally complex (solid solution)
CCA	complex concentrated alloy
HE	high entropy (solid solution)
HEA	high entropy alloy
HPT	high pressure turbine
HT	heat treated
NICE	Niobium Intermetallic Composite Elaboration
RM	refractory metal
RCCA	refractory complex concentrated alloy
RHEA	refractory high entropy alloy
RMIC	refractory metal intermetallic composite
RMIC/RHEA	RMIC that is also RHEA
RM(Nb)IC	refractory metal intermetallic composite based on Nb
RM(Nb)IC/RCCA	RM(Nb)IC that is also RCCA
RM(Nb)IC/RHEA	RM(Nb)IC that is also RHEA
TM	transition metal
UHTM	ultra-high temperature material
VEC	valence electron concentration

Appendix B. Nominal Compositions (at.%) of Reference Alloys Used in this Work

Alloy	Nb	Ti	Si	Al	B	Hf	Cr	Mo	Ta	V	W	Ge	Sn	Ref.
EZ8	43	24	18	5	-	5	5	-	-	-	-	-	5	[80]
JG3	46	24	18	5	-	-	5	2	-	-	-	-	-	[83]
JG4	41	24	18	5	-	5	5	2	-	-	-	-	-	[86]
JG6	36	24	18	5	-	5	5	2	-	-	-	-	5	[86]
JN1	43	24	18	5	-	5	5	-	-	-	-	-	-	[76]
JN2	43	15	18	-	-	2	10	5	-	-	5	-	2	[87]
JN3	51	15	18	-	-	2	2	5	-	-	5	-	2	[87]
JN4	45	20	20	-	-	2	2	6	-	-	-	-	5	[87]
JZ3	41.8	12.4	17.7	4.7	-	1	5.2	-	6	-	2.7	4.8	3.7	[66]
JZ3+	38.7	12.4	19.7	4.6	-	0.8	5.2	-	5.7	-	2.3	4.9	5.7	[66]
JZ4 *	38.9	12.5	17.8	5	-	1.1	5.2	6.2	-	-	2.3	5.2	5.8	[67]
JZ5 *	32	20.4	19.2	4.5	-	0.9	4.7	6.3	-	-	1.1	5.2	5.7	[67]
KZ5	48	24	18	5	-	-	5	-	-	-	-	-	-	[81]
KZ6	42	24	18	5	–	-	5	-	6	-	-	-	-	[82]
OHS1	38	24	18	5	-	-	5	-	-	-	-	5	5	[65]
NV1	53	23	5	5	-	5	2	-	-	5	-	-	2	[50]
TT4 *	42.4	24.6	15.7	5	6.9	-	5.4	-	-	-	-	-	-	[61]
TT5	37	24	18	5	5	-	5	-	6	-	-	-	-	[62]
TT6	39	24	18	4	6	-	5	-	-	-	-	-	4	[62]
TT7	38	24	17	5	6	5	5	-	-	-	-	-	-	[62]
TT8	42.5	24	17	3.5	6	5	2	-	-	-	-	-	-	[61]
ZF6	43	24	18	5	-	-	5	-	-	-	-	5	-	[64]
ZF9	38	24	18	5	-	5	5	-	-	-	-	5	-	[64]
ZX8	43	24	18	5	-	-	5	-	-	-	-	-	5	[58]

* actual composition.

References

1. Tsakiropoulos, P. Alloys for application at ultra-high temperatures: Nb-silicide in situ composites. Challenges, breakthroughs and opportunities. *Prog. Mater. Sci.* **2022**, *123*, 100714. [CrossRef]
2. Tsakiropoulos, P. Refractory Metal Intermetallic Composites, High-Entropy Alloys, and Complex Concentrated Alloys: A Route to Selecting Substrate Alloys and Bond Coat Alloys for Environmental Coatings. *Materials* **2022**, *15*, 2832. [CrossRef] [PubMed]
3. Senkov, O.N.; Miracle, D.B.; Chaput, K.J.; Couzinie, J.-P. Development and exploration of refractory high entropy alloys—A review. *J. Mater. Res.* **2018**, *33*, 3092–3128. [CrossRef]
4. Gorsse, S.; Couzinié, J.-P.; Miracle, D.B. From high-entropy alloys to complex concentrated alloys. *Comptes Rendus Phys.* **2018**, *19*, 721–736. [CrossRef]
5. Jia, Y.; Jia, Y.; Wu, S.; Ma, X.; Wang, G. Novel Ultralight-Weight Complex Concentrated Alloys with High Strength. *Materials* **2019**, *12*, 1136. [CrossRef]
6. Liu, H.; Liu, L.; Xin, C. Effect of alloying elements on the structure and mechanical properties of NbMoTaWX (X = Cr, V, Ti, Zr, and Hf) refractory high-entropy alloys. *AIP Adv.* **2021**, *11*, 025044. [CrossRef]
7. Senkov, O.N.; Tsakiropoulos, P.; Couzinié, J.-P. Special Issue "Advanced Refractory Alloys": Metals, MDPI. *Metals* **2022**, *12*, 333. [CrossRef]
8. Bewlay, B.P.; Jackson, M.R.; Subramanian, P.R.; Lewandowski, J.J. Very high temperature Nb silicide based composites, in Niobium for High Temperature Applications, Edited by Young-Won Kim and Tadeu Carneiro. *TMS (Miner. Met. Mater. Soc.)* **2004**, 51–61.
9. Jackson, M.; Subramanian, P.; Zhao, J.-C.; Bewlay, B.; Darolia, R.; Schafrick, R. Turbine Blade for Extreme Temperature Conditions. Patent Application US 2004/0126327 A1, 1 July 2004.

10. Bewlay, B.P.; Darolia, R.; Dheeradhada, V.S.; DiDomizio, R.; Gigliotti, M.F.X.; Rigney, J.D.; Subramanian, P.R. Nb-Si Based Alloys Having an Al-Containing Coating, Articles and Processes. Patent Application US 2009/0042054 A1, 12 February 2009.
11. Bewlay, B.P.; Subramanian, P.R.; Rigney, J.D.; DiDomizio, R.; Dheeradhada, V.S. Oxide Forming Protective Coatings for Niobium Based Materials. Patent Application US 2012/0282485 A1, 8 November 2012.
12. Sun, J.; Fu, Q.-G.; Guo, L.-P.; Wang, L. Silicide Coating Fabricated by HAPC/SAPS Combination to Protect Niobium Alloy from Oxidation. *ACS Appl. Mater. Interfaces* **2016**, *8*, 15838–15847. [CrossRef]
13. Perepezko, J.H. Environmental Resistant Coatings for High Temperature Mo and Nb Silicide Alloys. *MRS Adv.* **2017**, *2*, 1323–1334. [CrossRef]
14. Sun, Z.; Tian, X.; Guo, X.; Yin, M.; Zhang, F.; Zhang, X. Oxidation resistance and mechanical characterization of silicide coatings on the Nb-18Ti-14Si-9Al alloy. *Int. J. Refract. Met. Hard Mater.* **2017**, *69*, 18–26. [CrossRef]
15. Ghadyani, M.; Utton, C.; Tsakiropoulos, P. Microstructures and Isothermal Oxidation of the Alumina Scale Forming Nb1.7Si2.4Ti2.4Al3Hf0.5 and Nb1.3Si2.4Ti2.4Al3.5Hf0.4 Alloys. *Materials* **2019**, *12*, 222. [CrossRef] [PubMed]
16. Ghadyani, M.; Utton, C.; Tsakiropoulos, P. Microstructures and Isothermal Oxidation of the Alumina Scale Forming Nb1.45Si2.7Ti2.25Al3.25Hf0.35 and Nb1.35Si2.3Ti2.3Al3.7Hf0.35 Alloys. *Materials* **2019**, *12*, 759. [CrossRef]
17. Hernández-Negrete, O.; Tsakiropoulos, P. On the Microstructure and Isothermal Oxidation at 800, 1200, and 1300 °C of the Al-25.5Nb-6Cr-0.5Hf (at %) Alloy. *Materials* **2019**, *12*, 2531. [CrossRef]
18. Zhang, X.; Fu, T.; Cui, K.; Zhang, Y.; Shen, F.; Wang, J.; Yu, L.; Mao, H. The Protection, Challenge, and Prospect of Anti-Oxidation Coating on the Surface of Niobium Alloy. *Coatings* **2021**, *11*, 742. [CrossRef]
19. Grilli, M.L.; Valerini, D.; Slobozeanu, A.E.; Postolnyi, B.O.; Balos, S.; Rizzo, A.; Piticescu, R.R. Critical Raw Materials Saving by Protective Coatings under Extreme Conditions: A Review of Last Trends in Alloys and Coatings for Aerospace Engine Applications. *Materials* **2021**, *14*, 1656. [CrossRef]
20. Kim, W.-Y.; Yeo, I.-D.; Kim, M.-S.; Hanada, S. Effect of Cr Addition on Microstructure and Mechanical Properties in Nb-Si-Mo Base Multiphase Alloys. *Mater. Trans.* **2002**, *43*, 3254–3261. [CrossRef]
21. Su, L.F.; Jia, L.N.; Feng, Y.B.; Zhang, H.R.; Yuan, S.N.; Zhang, H. Microstructure and room-temperature fracture toughness of directionally solidified Nb-Si-Ti-Cr-Al-Hf alloy. *Mater. Sci. Eng. A* **2013**, *560*, 672–677. [CrossRef]
22. Zhang, S.; Guo, X. Alloying effects on the microstructure and properties of Nb–Si based ultrahigh temperature alloys. *Intermetallics* **2016**, *70*, 33–44. [CrossRef]
23. Sheng, L.Y.; Tian, Y.X.; Guo, J.T. Microstructural Characteristics and Mechanical Properties of a Nb/Nb_5Si_3 based Composite with and without Directional Solidification. *Adv. Compos. Lett.* **2018**, *27*, 096369351802700405. [CrossRef]
24. Tsakiropoulos, P. On Nb Silicide Based Alloys: Alloy Design and Selection. *Materials* **2018**, *11*, 844. [CrossRef] [PubMed]
25. Lee, S.Y.; Park, K.B.; Kang, J.-W.; Kim, Y.; Kang, H.-S.; Ha, T.K.; Min, S.-H.; Park, H.-K. Spark Plasma Sintering Behavior of Nb-Mo-Si Alloy Powders Fabricated by Hydrogenation-Dehydrogenation Method. *Materials* **2019**, *12*, 3549. [CrossRef] [PubMed]
26. Ma, R.; Guo, X. Composite alloying effects of V and Zr on the microstructures and properties of multi-elemental Nb–Si based ultrahigh temperature alloys. *Mater. Sci. Eng. A* **2021**, *813*, 141175. [CrossRef]
27. Tsakiropoulos, P. Refractory Metal (Nb) Intermetallic Composites, High Entropy Alloys, Complex Concentrated Alloys and the Alloy Design Methodology NICE—Mise-en-scène † Patterns of Thought and Progress. *Materials* **2021**, *14*, 989. [CrossRef]
28. Lemberg, J.A.; Ritchie, R.O. Mo-Si-B Alloys for Ultrahigh-Temperature Structural Applications. *Adv. Mater.* **2012**, *24*, 3445–3480. [CrossRef] [PubMed]
29. Shah, D.M.; Berczik, D.; Anton, D.L.; Hecht, R. Appraisal of other silicides as structural materials. *Mater. Sci. Eng. A* **1992**, *155*, 45–57. [CrossRef]
30. Petrovic, J.J.; Vasudevan, A.K. Overview of High Temperature Structural Silicides. *MRS Proc.* **1993**, *322*, 3–8. [CrossRef]
31. Bewlay, B.P.; Whiting, P.W.; Davis, A.W.; Briant, C.L. Creep Mechanisms in Niobium-Silicide Based In-Situ Composites. *MRS Proc.* **1998**, *552*, 6111. [CrossRef]
32. Petrovic, J.J.; Vasudevan, A.K. Key developments in high temperature structural silicides. *Mater. Sci. Eng. A* **1999**, *261*, 1–5. [CrossRef]
33. Chu, F.; Thoma, D.J.; McClellan, K.J.; Peralta, P. Mo5Si3 single crystals: Physical properties and mechanical behaviour. *Mat. Sci. Eng. A* **1999**, *261*, 44–52. [CrossRef]
34. Yi, D.Q.; Du, R.X.; Cao, Y. Physical metallurgy of M5Si3-type silicides. *Acta Metall. Sin.* **2001**, *37*, 1121–1130.
35. Jackson, M.R.; Bewlay, B.P.; Briant, C.L. Creep Resistant Nb-Silicide Based Two-Phase Composites. U.S. Patent 6447623 B1, 10 September 2002.
36. Kim, J.H.; Tabaru, T.; Hirai, H. Tensile and Creep Properties of the Refractory Nb Base In-Situ Composite. *Int. J. Mod. Phys. B* **2003**, *17*, 1608–1614. [CrossRef]
37. Chen, Y.; Shang, J.-X.; Zhang, Y. Bonding characteristics and site occupancies of alloying elements in different Nb5Si3 phases from first principles. *Phys. Rev. B* **2007**, *76*, 184204. [CrossRef]
38. Tao, X.; Jund, P.; Colinet, C.; Tedenac, J.-C. Phase stability and physical properties of Ta5Si3 compounds from first-principles calculations. *Phys. Rev. B* **2009**, *80*, 104103. [CrossRef]
39. Tao, X.; Jund, P.; Colinet, C.; Tédenac, J.-C. First-principles study of the structural, electronic and elastic properties of W5Si3. *Intermetallics* **2010**, *18*, 688–693. [CrossRef]

40. Tsakiropoulos, P. On the Alloying and Properties of Tetragonal Nb5Si3 in Nb-Silicide Based Alloys. *Materials* **2018**, *11*, 69. [CrossRef] [PubMed]
41. Cockeram, B.; Saqib, M.; Srinivasan, R.; Weiss, I. Role of Nb3Si in high temperature deformation of a cast Nb-10 a/o Si in-situ composite. *Scr. Met. Mater.* **1992**, *26*, 749–754. [CrossRef]
42. Bewlay, B.P.; Jackson, M.R.; Zhao, J.-C.; Subramanian, P.R.; Mendiratta, M.G.; Lewandowski, J.J. Ultrahigh-Temperature Nb-Silicide-Based Composites. *MRS Bull.* **2003**, *28*, 646–653. [CrossRef]
43. Yurchenko, N.; Stepanov, N.; Salishchev, G. Laves-phase formation criterion for high-entropy alloys. *Mater. Sci. Technol.* **2017**, *33*, 17–22. [CrossRef]
44. Tsakiropoulos, P. Alloying and Properties of C14–NbCr2 and A15–Nb3X (X = Al, Ge, Si, Sn) in Nb–Silicide-Based Alloys. *Materials* **2018**, *11*, 395. [CrossRef]
45. Yeh, C.-L.; Chen, Y.-C. Formation of Mo5Si3/Mo3Si–MgAl2O4 Composites via Self-Propagating High-Temperature Synthesis. *Molecules* **2019**, *25*, 83. [CrossRef] [PubMed]
46. Bewlay, B.P.; Lipsitt, H.A.; Reeder, W.J.; Jackson, M.R.; Sutliff, J.A. Toughening mechanisms in directionally solidified Nb-Nb3Si-Nb5Si3 in-situ composites. In *Processing and Fabrication of Advanced Materials III*; Ravi, V.A., Srivatsan, T.S., Moore, J.J., Eds.; The Minerals Metals and Materials Society: Warrendale, PA, USA, 1994; pp. 547–565.
47. Huang, Q.; Guo, X.-P.; Kang, Y.-W.; Song, J.-X.; Qu, S.-Y.; Han, Y.-F. Microstructures and mechanical properties of directionally solidified multi-element Nb-Si alloy. *Prog. Nat. Sci. Mater. Int.* **2011**, *21*, 146–152. [CrossRef]
48. Wang, J.; Jia, L.; Ma, L.; Yuan, S.; Zhang, X.; Zhang, H. Microstructure optimisation of directionally solidified hypereutectic Nb-Si alloy. *Trans. Nonferr. Met. Soc. China* **2013**, *23*, 2874–2881. [CrossRef]
49. Tsakiropoulos, P. Alloying and Hardness of Eutectics with Nbss and Nb5Si3 in Nb-silicide Based Alloys. *Materials* **2018**, *11*, 592. [CrossRef] [PubMed]
50. Vellios, N.; Keating, P.; Tsakiropoulos, P. On the Microstructure and Properties of the Nb-23Ti-5Si-5Al-5Hf-5V-2Cr-2Sn (at.%) Silicide-Based Alloy—RM(Nb)IC. *Metals* **2021**, *11*, 1868. [CrossRef]
51. Vellios, N.; Tsakiropoulos, P. The Effect of Fe Addition in the RM(Nb)IC Alloy Nb–30Ti–10Si–2Al–5Cr–3Fe–5Sn–2Hf (at.%) on Its Microstructure, Complex Concentrated and High Entropy Phases, Pest Oxidation, Strength and Contamination with Oxygen, and a Comparison with Other RM(Nb)ICs, Refractory Complex Concentrated Alloys (RCCAs) and Refractory High Entropy Alloys (RHEAs). *Materials* **2022**, *15*, 5815. [CrossRef]
52. Liu, C.M.; Wang, H.M.; Zhang, S.Q.; Tang, H.B.; Zhang, A.L. Microstructure and oxidation behavior of new refractory high entropy alloys. *J. Alloys Compd.* **2014**, *583*, 162–169. [CrossRef]
53. Guo, N.; Wang, L.; Luo, L.; Li, X.; Chen, R.; Su, Y.; Guo, J.; Fu, H. Microstructure and mechanical properties of refractory high entropy (Mo 0.5 NbHf 0.5 ZrTi) BCC /M 5 Si 3 in-situ compound. *J. Alloys Compd.* **2016**, *660*, 197–203. [CrossRef]
54. Liu, Y.; Zhang, Y.; Zhang, H.; Wang, N.; Chen, X.; Zhang, H.; Li, Y. Microstructure and mechanical properties of refractory HfMo0.5NbTiV0.5Six high-entropy composites. *J. Alloys Compd.* **2017**, *694*, 869–876. [CrossRef]
55. Tsakiropoulos, P. On the Nb silicide based alloys: Part I—The bcc Nb solid solution. *J. Alloys Compd.* **2017**, *708*, 961–971. [CrossRef]
56. Tsakiropoulos, P. On the stability of complex concentrated (CC)/high entropy (HE) solid solutions and the contamination with oxygen of solid solutions in refractory metal intermetallic composites (RM(Nb)ICs) and refractory complex concentrated alloys (RCCAs). *Materials* **2022**, *15*, 8479. [CrossRef] [PubMed]
57. Xu, Z.; Utton, C.; Tsakiropoulos, P. A study of the effect of 2 at.% Sn on the microstructure and isothermal oxidation at 800 and 1200 °C of Nb-24Ti-18Si based alloys with Al and/or Cr additions. *Materials* **2018**, *11*, 1826. [CrossRef] [PubMed]
58. Xu, Z.; Utton, C.; Tsakiropoulos, P. A study of the effect of 5 at.% Sn on the microstructure and isothermal oxidation at 800 and 1200 °C of Nb-24Ti-18Si based alloys with Al and/or Cr additions. *Materials* **2020**, *13*, 245. [CrossRef] [PubMed]
59. Li, Z.; Tsakiropoulos, P. The Effect of Ge Addition on the Oxidation of Nb-24Ti-18Si Silicide Based Alloys. *Materials* **2019**, *12*, 3120. [CrossRef] [PubMed]
60. Tsai, M.-H.; Yeh, J.-W. High-entropy alloys: A critical review. *Mater. Res. Lett.* **2014**, *2*, 107–123. [CrossRef]
61. Thandorn, T.; Tsakiropoulos, P. The effect of Boron on the microstructure and properties of refractory metal intermetallic composites (RM(Nb)ICs) based on Nb-24Ti-xSi (x = 16, 17 or 18 at.%) with additions of Al, Cr or Mo. *Materials* **2021**, *14*, 6101. [CrossRef]
62. Thandorn, T.; Tsakiropoulos, P. On the microstructure and properties of Nb-Ti-Cr-Al-B-Si-X (X = Hf, Sn, Ta) refractory complex concentrated alloys. *Materials* **2021**, *14*, 7615. [CrossRef]
63. Schlesinger, M.E.; Okamoto, H.; Gokhale, A.B.; Abbaschian, R. The Nb-Si (Niobium-Silicon) System. *J. Phase Equilib. Diffus.* **1993**, *14*, 502–509. [CrossRef]
64. Li, Z.; Tsakiropoulos, P. On the microstructure and hardness of the Nb-24Ti-18Si-5Al-5Cr-5Ge and Nb-24Ti-18Si-5Al-5Cr-5Ge-5Hf (at.%) silicide based alloys. *Materials* **2019**, *12*, 2655. [CrossRef]
65. Hernandez-Negrete, O.; Tsakiropoulos, P. On the microstructure and isothermal oxidation at 800 and 1200 °C of the Nb-24Ti-18Si5Al-5Cr-5Ge-5Sn (at.%) silicide based alloy. *Materials* **2020**, *13*, 722. [CrossRef]
66. Zhao, J.; Utton, C.; Tsakiropoulos, P. On the Microstructure and Properties of Nb-12Ti-18Si-6Ta-5Al-5Cr-2.5W-1Hf (at.%) Silicide-Based Alloys with Ge and Sn Additions. *Materials* **2020**, *13*, 3719. [CrossRef] [PubMed]
67. Zhao, J.; Utton, C.; Tsakiropoulos, P. On the microstructure and properties of Nb-18Si-6Mo-5Al-5Cr-2.5W-1Hf Nb-Silicide based alloys with Ge, Sn and Ti additions (at.%). *Materials* **2020**, *13*, 4548. [CrossRef] [PubMed]

68. Bewlay, B.P.; Sitzman, S.D.; Brewer, L.N.; Jackson, M.R. Analyses of eutectoid phase transformations in Nb-silicide in-situ composites. *Microsc. Microanal.* **2004**, *10*, 470–480. [CrossRef] [PubMed]
69. Zhang, R.-Z.; Reece, M.J. Review of high entropy ceramics: Design, synthesis, structure and properties. *J. Mater. Chem. A* **2019**, *7*, 22148–22162. [CrossRef]
70. Shivakumar, S.; Qin, M.; Zhang, D.; Hu, C.; Yan, Q.; Luo, J. A new type of compositionally complex M5Si3 silicides: Cation ordering and unexpected phase stability. *Scr. Mater.* **2022**, *212*, 114557. [CrossRef]
71. Qin, Y.; Liu, J.X.; Li, F.; Wei, X.; Wu, H.; Zhang, G.J. A high entropy silicide by reactive spark plasma sintering. *J. Adv. Ceram.* **2019**, *8*, 148–152. [CrossRef]
72. Wright, A.J.; Wang, Q.; Huang, C.; Nieto, A.; Chen, R.; Luo, J. From high-entropy ceramics to compositionally-complex ceramics: A case study of fluorite oxides. *J. Eur. Ceram. Soc.* **2020**, *40*, 2120–2129. [CrossRef]
73. Tsakiropoulos, P. On Nb silicide based alloys: Part II. *J. Alloys Compd.* **2018**, *748*, 569–576. [CrossRef]
74. Bewlay, B.P.; Braiant, C.L.; Sylven, E.T.; Jackson, M.R.; Xiao, G. Creep Studies of Monolithic Phases in Nb-Silicide Based In-Situ Composites. *MRS Proc.* **2001**, *646*, 161–166. [CrossRef]
75. Zhao, J.; Utton, C.; Tsakiropoulos, P. On the Microstructure and Properties of Nb-12Ti-18Si-6Ta-2.5W-1Hf (at.%) Silicide-Based Alloys with Ge and Sn Additions. *Materials* **2020**, *13*, 1778. [CrossRef]
76. Nelson, J.; Ghadyani, M.; Utton, C.; Tsakiropoulos, P. A Study of the Effects of Al, Cr, Hf, and Ti Additions on the Microstructure and Oxidation of Nb-24Ti-18Si Silicide Based Alloys. *Materials* **2018**, *11*, 1579. [CrossRef] [PubMed]
77. Zacharis, E.; Utton, C.; Tsakiropoulos, P. A Study of the Effects of Hf and Sn on the Microstructure, Hardness and Oxidation of Nb-18Si Silicide Based Alloys without Ti Addition. *Materials* **2018**, *11*, 2447. [CrossRef] [PubMed]
78. Hernández-Negrete, O.; Tsakiropoulos, P. On the Microstructure and Isothermal Oxidation of Silica and Alumina Scale Forming Si-23Fe-15Cr-15Ti-1Nb and Si-25Nb-5Al-5Cr-5Ti (at.%) Silicide Alloys. *Materials* **2019**, *12*, 1091. [CrossRef] [PubMed]
79. Hernández-Negrete, O.; Tsakiropoulos, P. On the Microstructure and Isothermal Oxidation of the Si-22Fe-12Cr-12Al-10Ti-5Nb (at.%) Alloy. *Materials* **2019**, *12*, 1806. [CrossRef] [PubMed]
80. Zacharis, E.; Utton, C.; Tsakiropoulos, P. A Study of the Effects of Hf and Sn on the Microstructure, Hardness and Oxidation of Nb-18Si Silicide-Based Alloys-RM(Nb)ICs with Ti Addition and Comparison with Refractory Complex Concentrated Alloys (RCCAs). *Materials* **2022**, *15*, 4596. [CrossRef]
81. Zelenitsas, K.; Tsakiropoulos, P. Study of the role of Cr and Al additions in the microstructure of Nb-Ti-Si in situ composites. *Intermetallics* **2005**, *13*, 1079–1095. [CrossRef]
82. Zelenitsas, K.; Tsakiropoulos, P. Study of the role of Ta and Cr additions in the microstructure of Nb-Ti-Si-Al in situ composites. *Intermetallics* **2006**, *14*, 639–659. [CrossRef]
83. Geng, J.; Tsakiropoulos, P.; Shao, G. The effects of Ti and Mo additions on the microstructure of Nb-silicide base in situ composites. *Intermetallics* **2006**, *14*, 227–235. [CrossRef]
84. Balasubramanian, K.; Khare, S.V.; Gall, D. Valence electron concentration as an indicator for mechan-ical properties in rock salt structure nitrides, carbides and carbo-nitrides. *Acta Mater.* **2018**, *152*, 175–185. [CrossRef]
85. Papadimitriou, I.; Utton, C.; Tsakiropoulos, P. The impact of Ti and temperature on the stability of Nb5Si3 phases: A first-principles study. *Sci. Technol. Adv. Mater.* **2017**, *18*, 467–479. [CrossRef]
86. Geng, J.; Tsakiropoulos, P.; Shao, G. A study of the effects of Hf and Sn additions on the microstructure of Nbss/Nb5Si3 based in situ composites. *Intermetallics* **2007**, *15*, 69–76. [CrossRef]
87. Nelson, J. Study of the Effects of Cr, Hf and Sn with Refractory Metal Additions on the Microstructure and Properties of Nb-Silicide Based Alloys. Ph.D. Thesis, University of Sheffield, Sheffield, UK, 2015.

Disclaimer/Publisher's Note: The statements, opinions and data contained in all publications are solely those of the individual author(s) and contributor(s) and not of MDPI and/or the editor(s). MDPI and/or the editor(s) disclaim responsibility for any injury to people or property resulting from any ideas, methods, instructions or products referred to in the content.